NASA CONTRACTOR REPORT

NASA CR - 61020

NASA CR - 61020

APOLLO LOGISTICS SUPPORT SYSTEMS MOLAB STUDIES

Task Report On

Mission Command and Control

Prepared under Contract No. NAS8-11096 by

Arch W. Meagher
Robert J. Bonham

NORTHROP SPACE LABORATORIES
Space Systems Section
6025 Technology Drive
Huntsville, Alabama

for

NASA - GEORGE C. MARSHALL SPACE FLIGHT CENTER
Huntsville, Alabama

October 1964

APOLLO LOGISTICS SUPPORT SYSTEMS
MOLAB STUDIES

Task Report On

Mission Command and Control

by

Arch W. Meagher
Robert J. Bonham

Prepared under Contract No. NAS8-11096 by

NORTHROP SPACE LABORATORIES

Space Systems Section

6025 Technology Drive

Huntsville, Alabama

For
ASTRIONICS LABORATORY

This report is reproduced photographically
from copy supplied by the contractor

NASA-GEORGE C. MARSHALL SPACE FLIGHT CENTER

Requests for copies of this report should be referred to

National Aeronautics and Space Administration
Office of Scientific and Technical Information
Attention: AFSS-A
Washington, D.C. 20546

PREFACE

This Technical Report, prepared by the Northrop Space Laboratories (NSL), Huntsville Department, for the George C. Marshall Space Flight Center under authorization of Task Order N-35, Contract NAS8-11096, is submitted on September 1, 1964.

The NASA Technical Representative was Mr. John F. Pavlick of the MSFC Astrionics Laboratory (R-ASTR-A).

The work completed was an eighteen man-week effort beginning on 1 July 1964, and ending 1 September 1964.

This report is herein submitted in two parts. Part I presents data which is the result of extrapolating dynamic analysis work done on MOLAB III to MOLAB VII. Part II presents equations generated for an ARTICULATED MOLAB. Part II of the task order represents a change from the original task order instituted by the Technical Representative.

INDEX OF ILLUSTRATIONS

TABLE OF CONTENTS

PART I

DYNAMIC STUDIES ON MOLAB VII

SECTION 1.0

INTRODUCTION

1.1 This section of the report includes the results of the extension of studies made on the MOLAB III Concept in Task Order N-22*. The results of the MOLAB III study are extrapolated to the MOLAB VII configuration where applicable.

The object of these studies was to investigate the stability of the MOLAB VII concept on sloping surfaces and to demonstrate the effect of C.G. height on limiting the stability under various conditions of surface, speed, and steering angles.

"Worst case" conditions have been used throughout the report in simulating possible lunar surface conditions. All bumps referred to in this report are 1/4 sine wave functions which take into consideration only minor wheel deformations.

Suspension constants used were 1,000 pounds per foot for springs and 250 pounds per foot damping.

The wheels were considered to have no damping and a spring constant of 1,000 pounds per foot. In the report on Task Order N-22* in which various suspension and tire constants were investigated for use on the MOLAB III configuration these constants were found to give the best over all results.

In this report a stable condition is defined as a condition or set of conditions under which the vehicle will not overturn; it does not infer that the condition is satisfactory. Roll and pitch angles, C. G. displacement, frequency of oscillations and control problems may make the vehicle untenable under stable conditions.

Figure 1 shows the characteristics of MOLAB VII and Figure 2 shows the conditions for this study.

1.2 PITCH PLANE STABILITY

1.2.1 CONDITIONS

The MOLAB was first examined for the case of striking a bump with both leading wheels to show the effect of C. G. height on the stability of the MOLAB under such conditions.

*This Task Order report is reference 1, Section 5. See Page for a brief explanation of Task Order N-22.

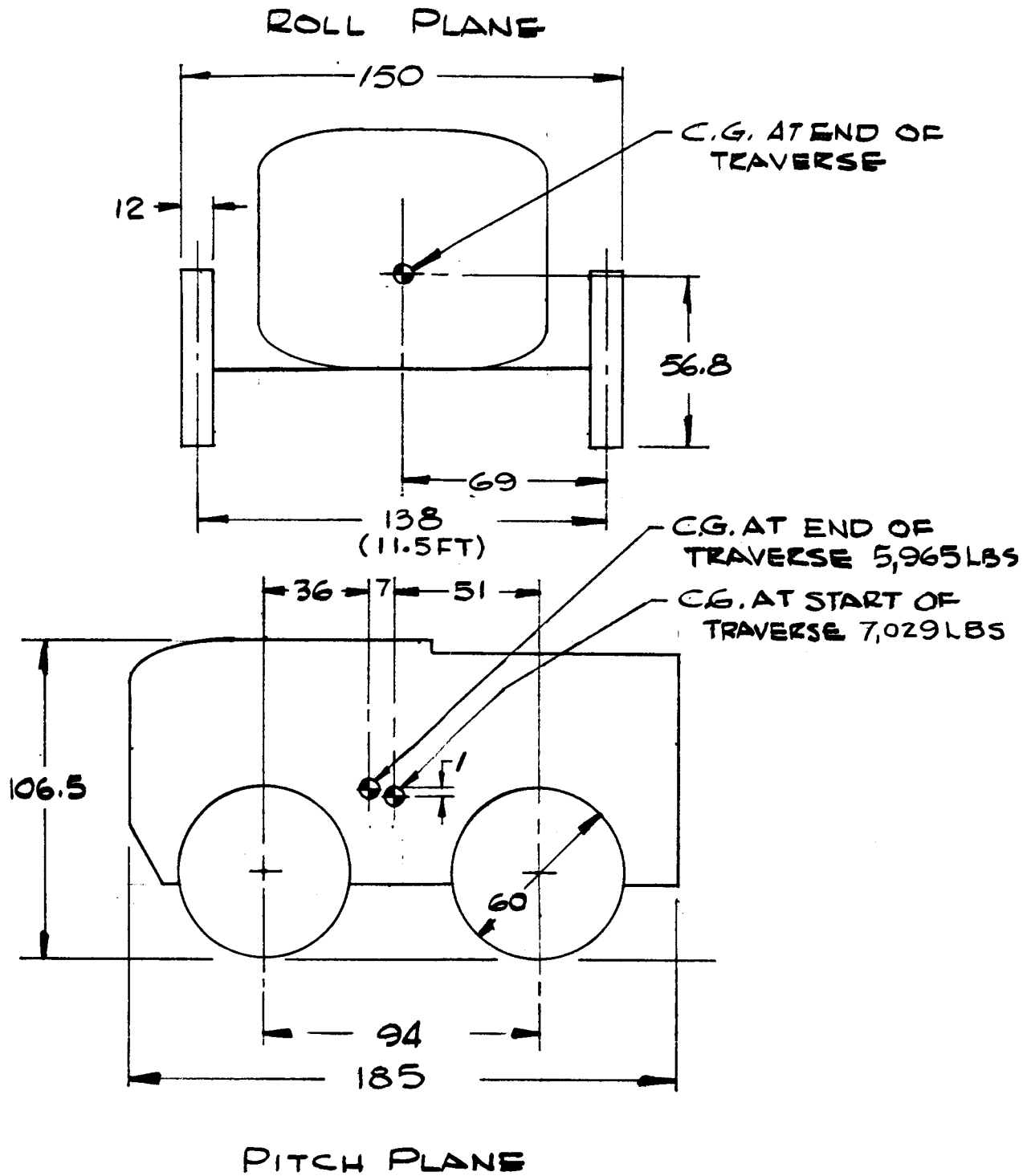

FIGURE 1. MOLAB VII CHARACTERISTICS

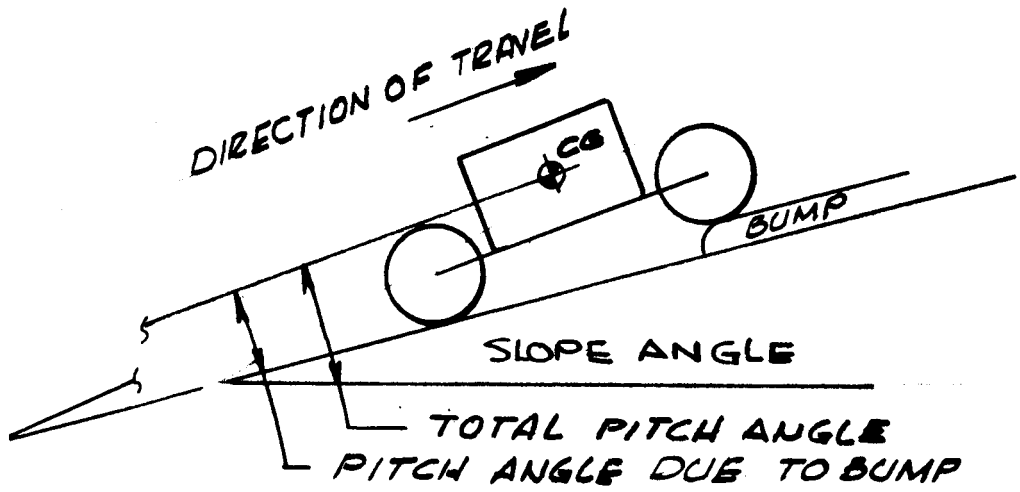

ROLL PLANE ANALYSIS STRIKING A BUMP

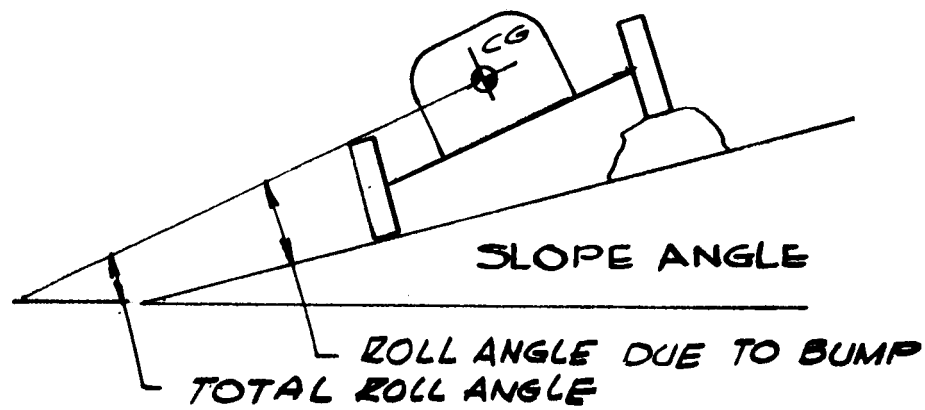

ROLL PLANE ANALYSIS DURING A TURN

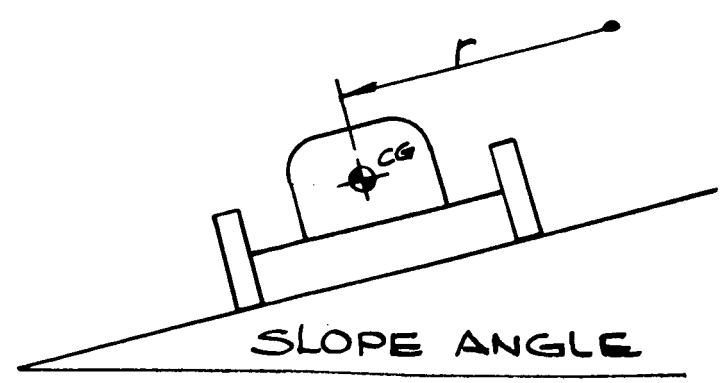

FIGURE 2. PITCH PLANE ANALYSIS

1.2.2 PROCEDURE

The pitch angles shown in Figure 3 were calculated by adding to the slope angle the pitch angle generated when the MOLAB VII vehicle, struck a bump on level ground as calculated in the report on Task Order N-22*. The dashed lines indicate points of instability for various C. G. heights.

1.2.3 RESULSTS

As may be seen from the graphs of Figure 3, the MOLAB VII has a smaller pitch angle when striking a given bump at high speeds than at low speed.

The characteristic is caused by the differences in time lag between when the front and rear wheels sequentially strike a bump at high and low speeds. At low speeds the front of the MOLAB will travel upward some time before the rear wheels strike the bump and start to rise resulting in a large pitch angle. However, at high speeds the rear of the vehicle will be affected by the bump before the pitch angle become large. Although the pitch angle is less for high speed the C. G. displacement is much greater at the higher speed.

As may be seen on the graphs of Figure 3 the MOLAB VII Configuration becomes unstable at 2.6 mph on a 10^{o} slope when striking a 1.75 foot bump. At 10.4 mph the MOLAB VII does not become unstable for the same bump until a slope of 20^{o} is reached. A trade off between pitch angle and C. G. displacement suggests a possible optimum speed for striking a bump on the lunar surface.

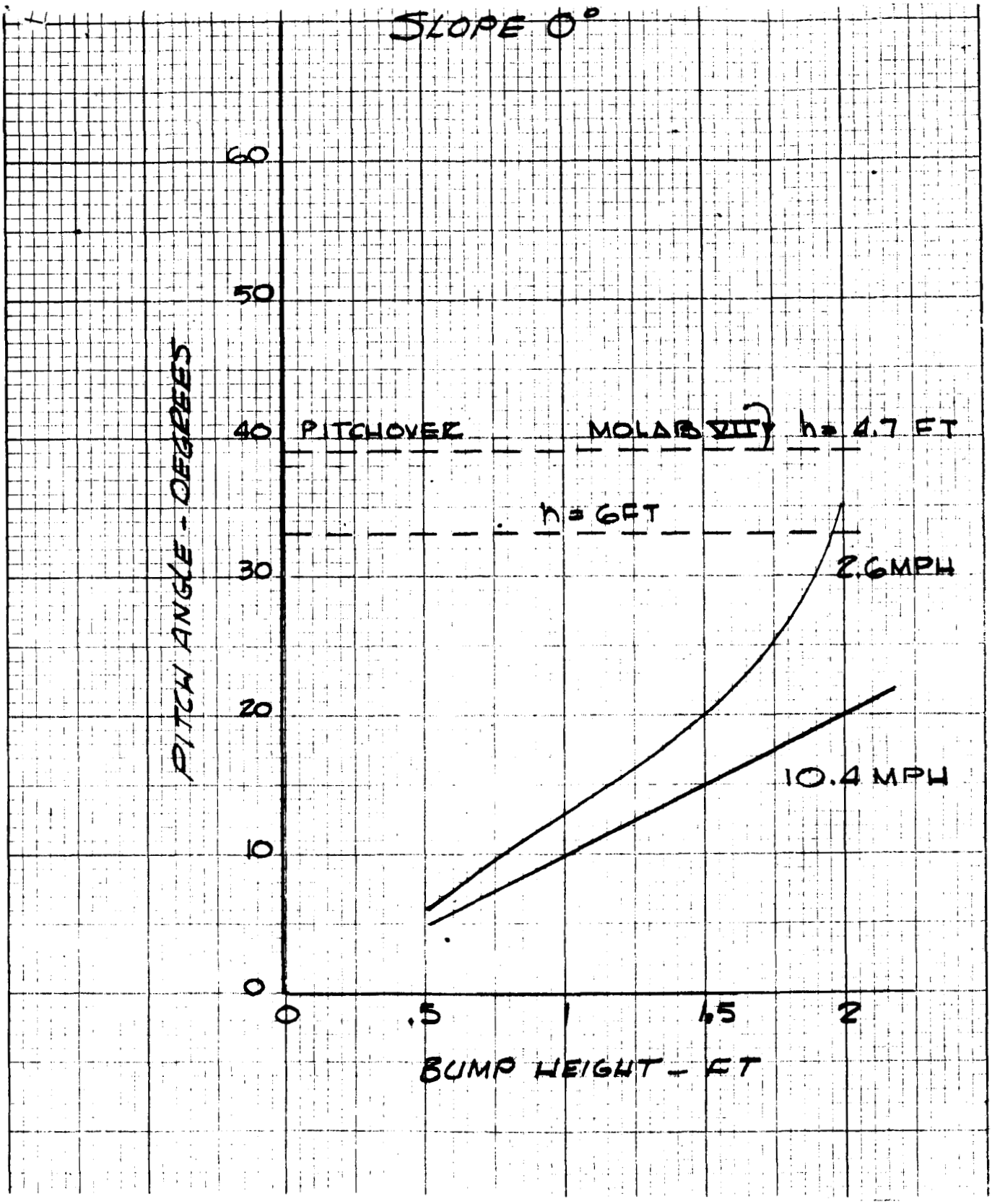

FIGURE 3A. PITCH PLANE STABILITY, SLOPE 0°

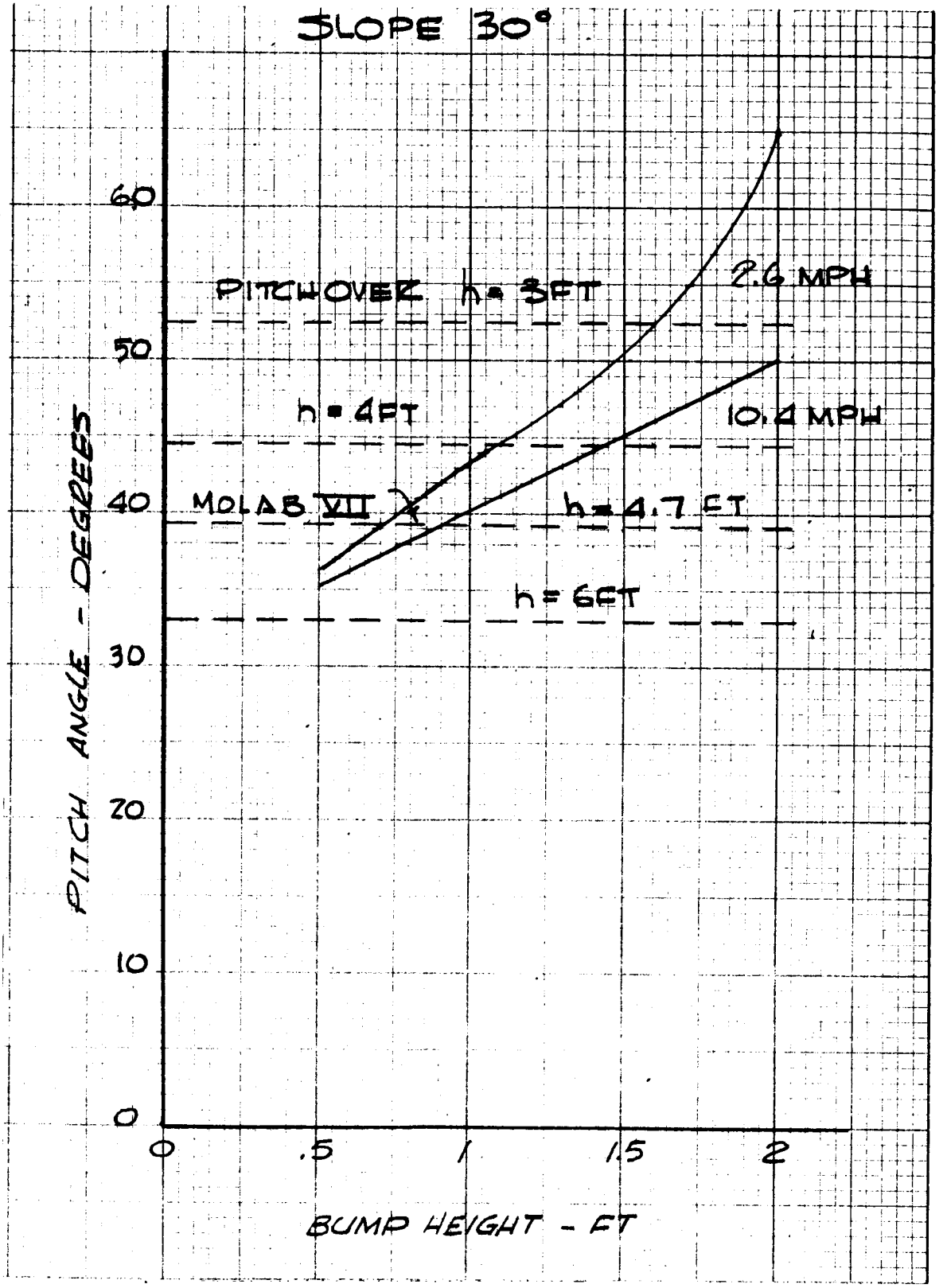

FIGURE 3D. PITCH PLANE STABILITY, SLOPE 30°

1.3 ROLL PLANE ANALYSIS

1.3.1 STRIKING AN OBSTACLE

1.3.1.1 Conditions

The MOLAB VII was analysed in the roll plane to demonstrate the effect of C. G. height on the MOLAB VII stability when the MOLAB strikes a bump with its up hill wheels while traveling along a slope as in Figure 2. Slopes of 0, 10, 20, and 30 degrees were used with bumps of .5,1, and 2 feet at speeds of 2.6 and 10.4 miles per hour.

1.3.1.2 Procedure

Roll angles were calculated by adding to the angle of the slope the vehicle roll angle produced when striking a bump on level ground as computed in the report on Task Order N-22*. Errors involved in this addition are small as long as the angles used are small.

In Figure 4 bump height versus roll angles is plotted for the conditions considered, roll over conditions for vehicles with C. G. heights of 3 to 6 feet are shown.

1.3.1.3 Results

As may be observed from the plots of Figure 4 the MOLAB VII is not well adopted for travel under the conditions considered. The MOLAB VII becomes unstable on a 20° slope when striking a 2 foot bump at approximately 5 mph and when striking a 1.75 foot bump at 5 mph on a 30° slope. If a safety factor of 2:1 were to be imposed for the roll angle, the MOLAB would be considered safe on a 20° slope for obstacles less than .5 feet at 5 mph and bumps of 1.5 feet high on a 10° slope at 5 mph. Under such conditions the mobility of the MOLAB VII would be restricted to comparatively smooth surface areas.

1.3.2 TURNING

1.3.2.1 Conditions

This portion of the report is intended to illustrate the effects of C. G. height and lunar surface conditions on the MOLAB VII while under going turns on sloping surfaces. The MOLAB VII was considered to be under going a U turn from a direction of down slope to up slope on slopes of 0, 10, 20, and 30 degrees.

1.3.2.2 Procedure

Figures 6 and 7 show the relationship between slope angles and

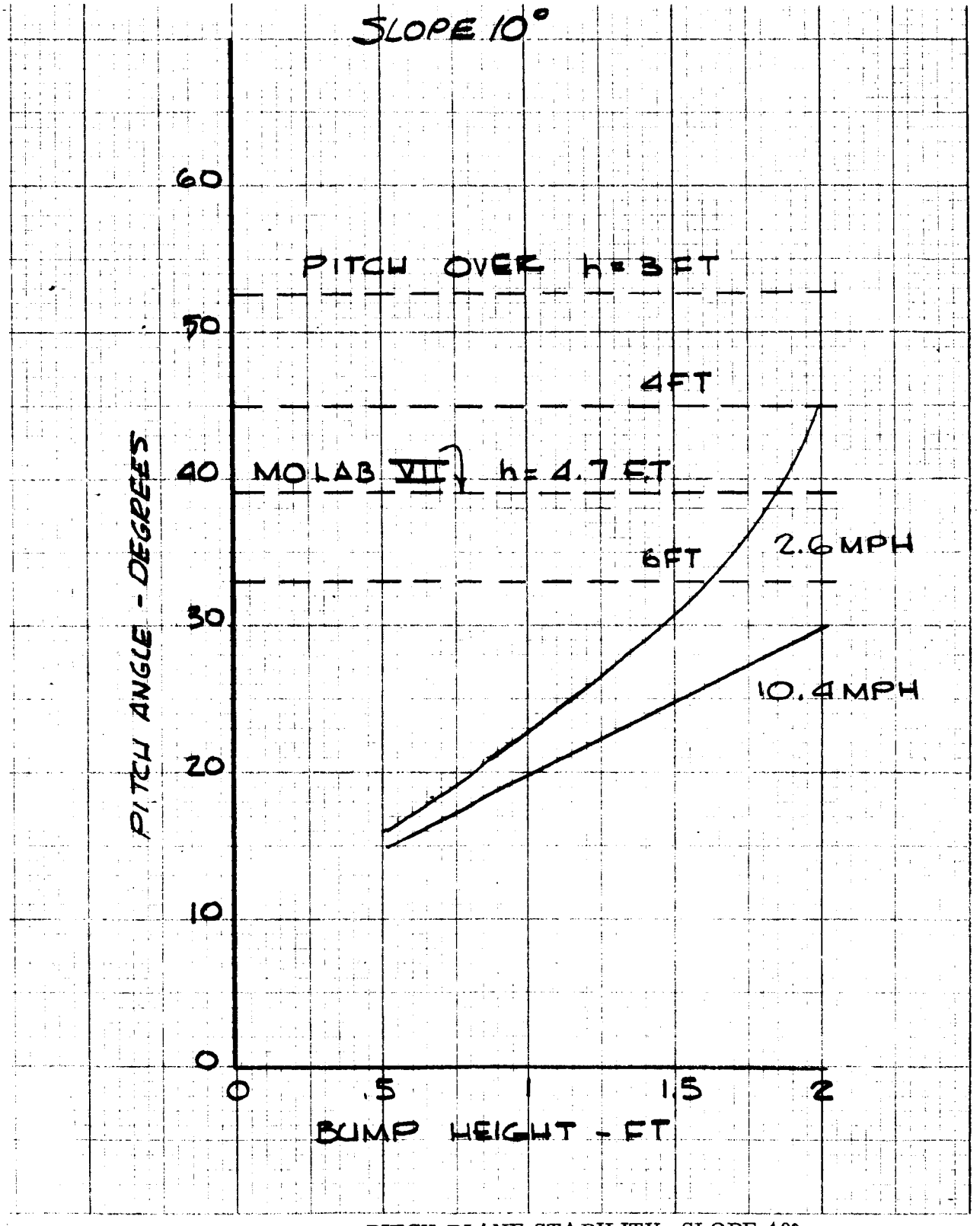

FIGURE 3B. PITCH PLANE STABILITY, SLOPE 10°

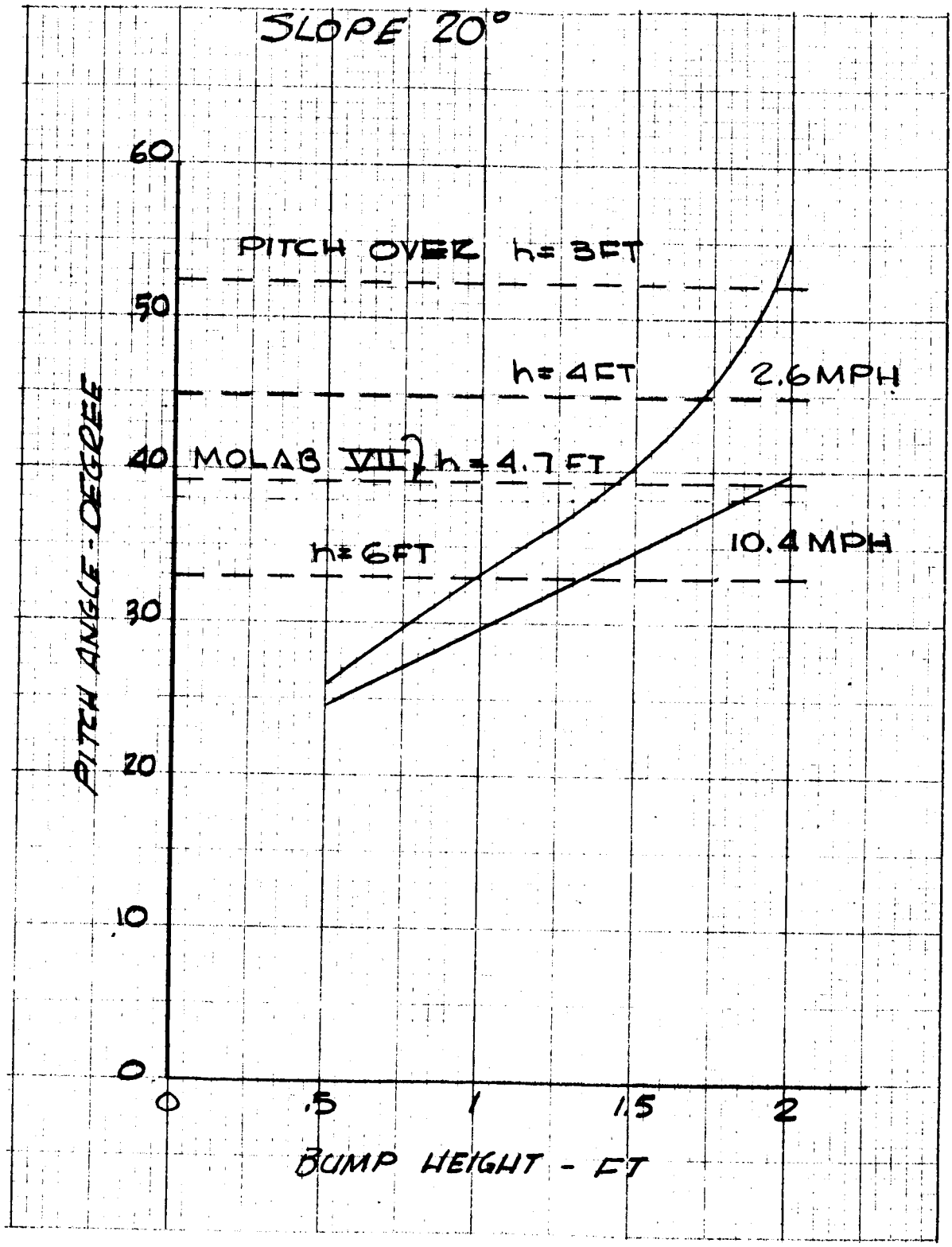

FIGURE 3C. PITCH PLANE STABILITY, SLOPE 20°

allowable steering angles. The limits imposed by the surface conditions are represented by the dashed lines. The MOLAB will skid if an attempt is made to operate the vehicle with conditions found below these lines. The solid lines are limits of steering angle and slope angle at a given speed. The MOLAB will overturn if operated above these limits if the surface conditions do not allow the vehicle to skid first.

The graphs were derived from data calculated in the report on Task Order N-22* for the MOLAB III having parameters simular to the MOLAB VII.

1.3.2.3 Results

As may be seen from Figures 5, 6 and 7 the MOLAB VII will skid before overturn for most value of expected to be found on the lunar surface. This conditions, although acting as a governor to prevent overturn during improperly executed turns, presents other problems. During the time the MOLAB is undergoing a skid, little if any control of the vehicle is possible. Collision with obstacles and the resulting possible damage is only one possibility. If, during a skid the MOLAB wheels strike an obstacle such as a crater rim or crevice, thereby bringing the skid to a sudden stop, a large moment will be produc ed tending to overturn the MOLAB. Because of the control problems during a skid and their possible serious results, skidding should be avoided.

1.4 CONCULUSIONS AND RECOMMENDATIONS

The stability of the MOLAB VII while operating on the lunar surface present serious probelems in the command and control of the vehicle and its subsystems as well as the overall mobility of the vehicle.

Major factors which contribute to the instability are the reduced lunar gravity, short wheel base, and high center of gravity. Although the lunar gravity is fixed, its effects to a degree can be compensated by the use of an active suspension system incorporating such features as controlled dampers and a vehicle leveling device. Such a system would represent a trade between increased stability and larger suspension weight and power requirements. The limits on wheel base are imposed by the delivery vehicle and MOLAB configuration. Every effort to make use of available space to improve the wheel base should be taken in order to obtain maximum performance from the MOLAB.

The location of the C. G. is very critical. The present height approximately five feet is too great for good stability. It is clear that any reduction in C. G. height is a major improvement in overall MOLAB stability. The active suspension system would lessen the effect of the high C. G. location but does not offer a total solution to

the problem.

*The report on Task Order N-22 is a dynamic analysis of the MOLAB III concept using a wide range of suspension and tire constants, steering methods, and worst case bump conditions on level ground. Data used in this report taken from N-22 is shown as 0^{o} slope conditions on the graphs.

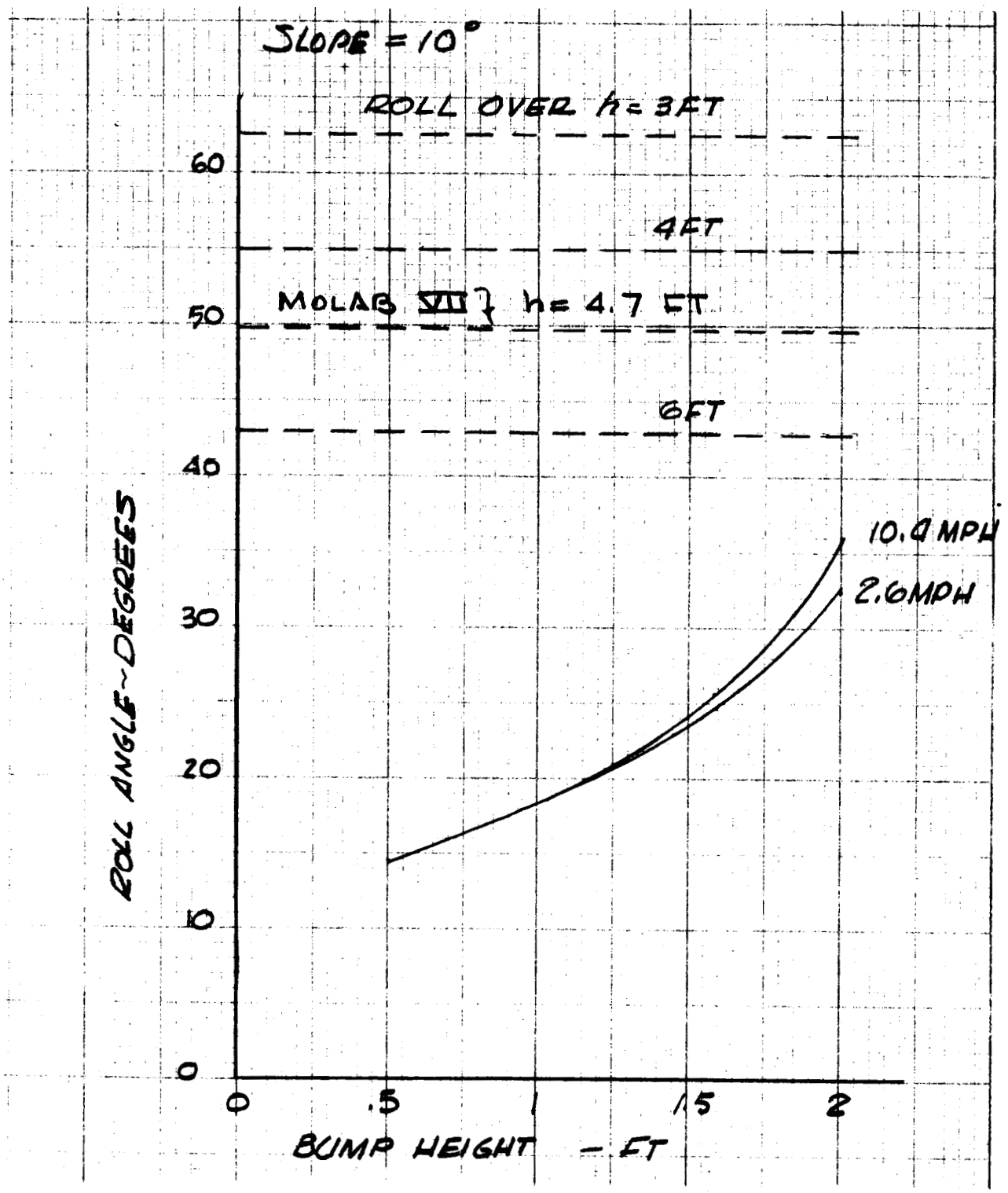

FIGURE 4B. ROLL PLANE STABILITY, SLOPE = 10°

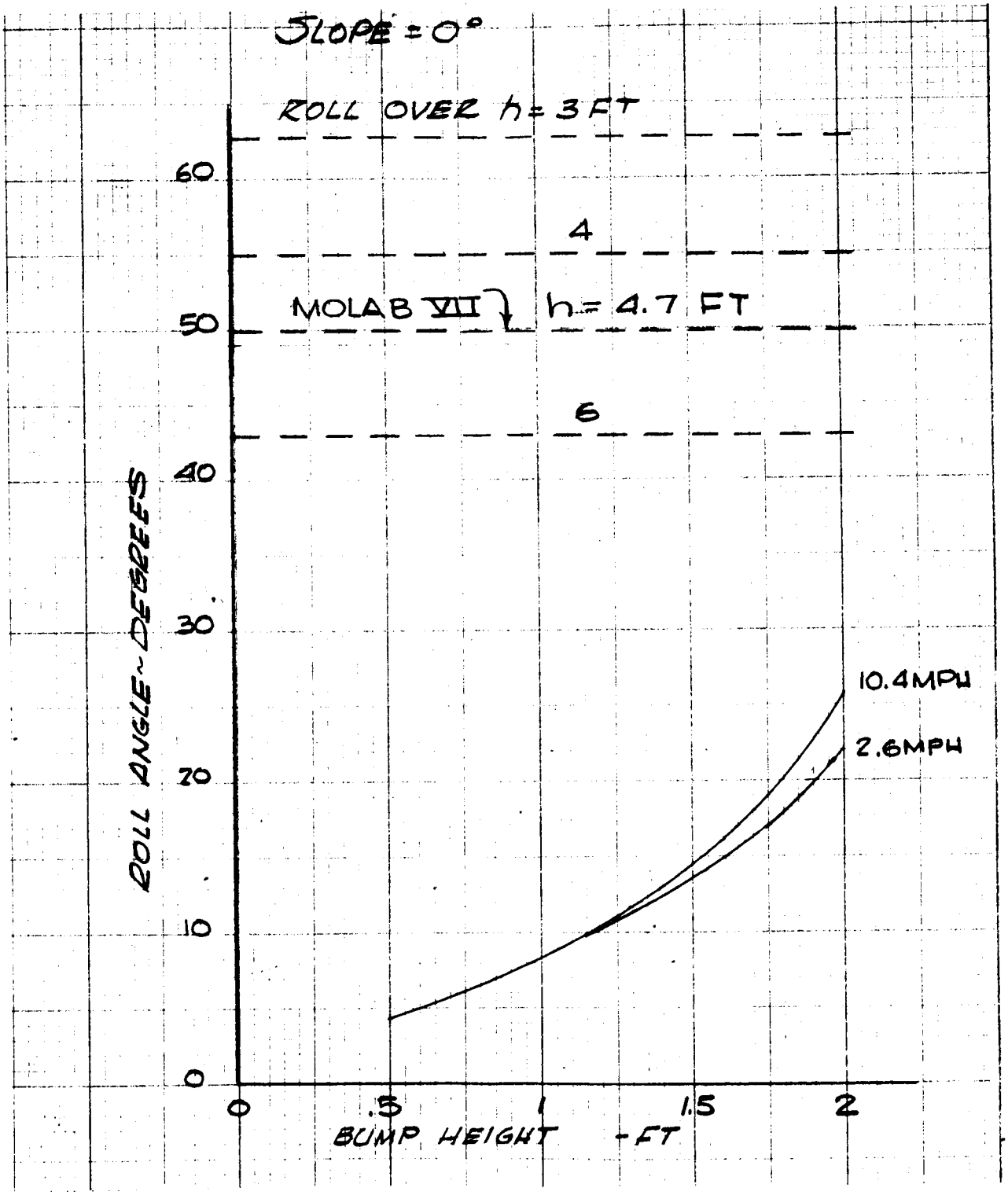

FIGURE 4A. ROLL PLANE STABILITY, SLOPE = 0°

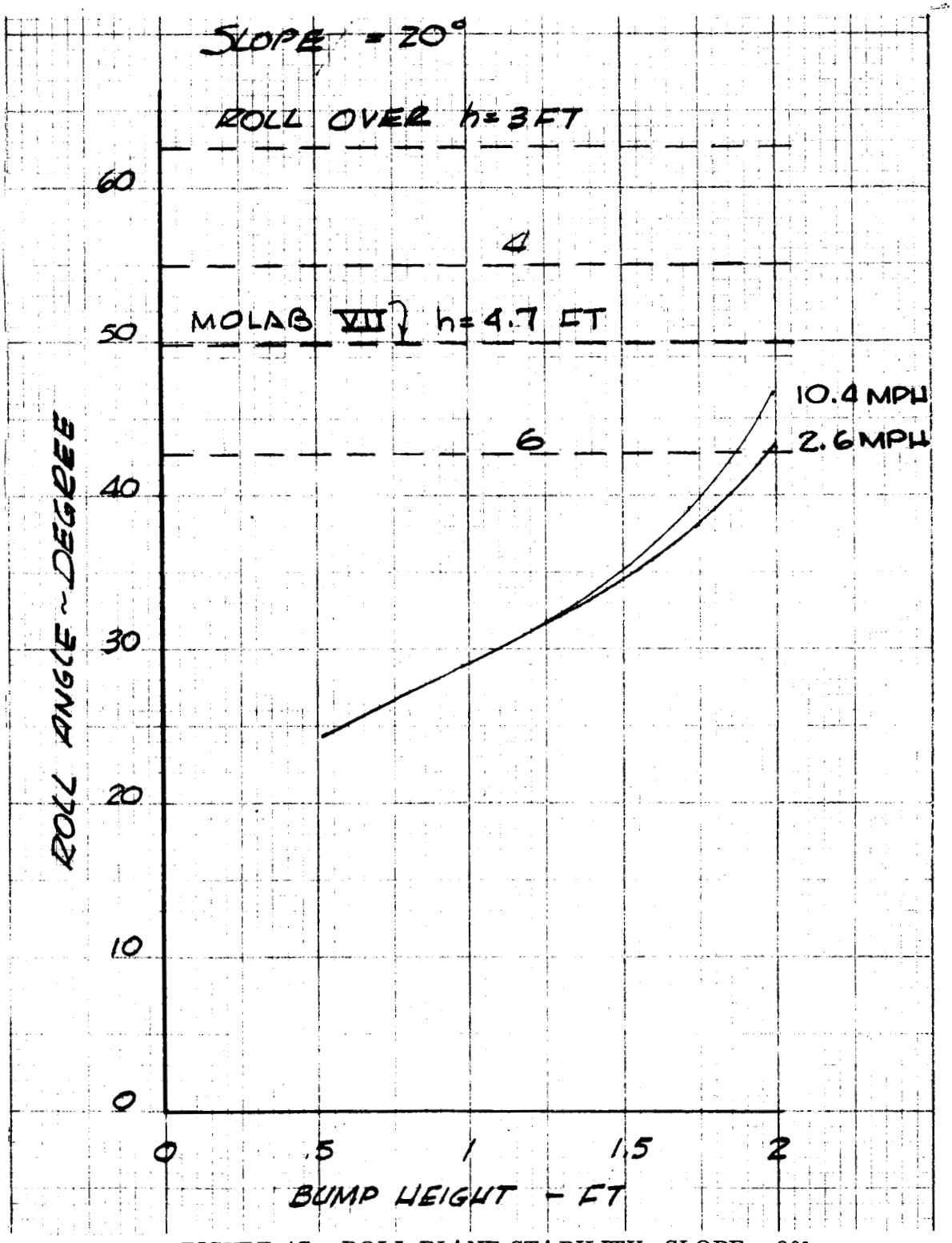

FIGURE 4C. ROLL PLANE STABILITY, SLOPE = 20°

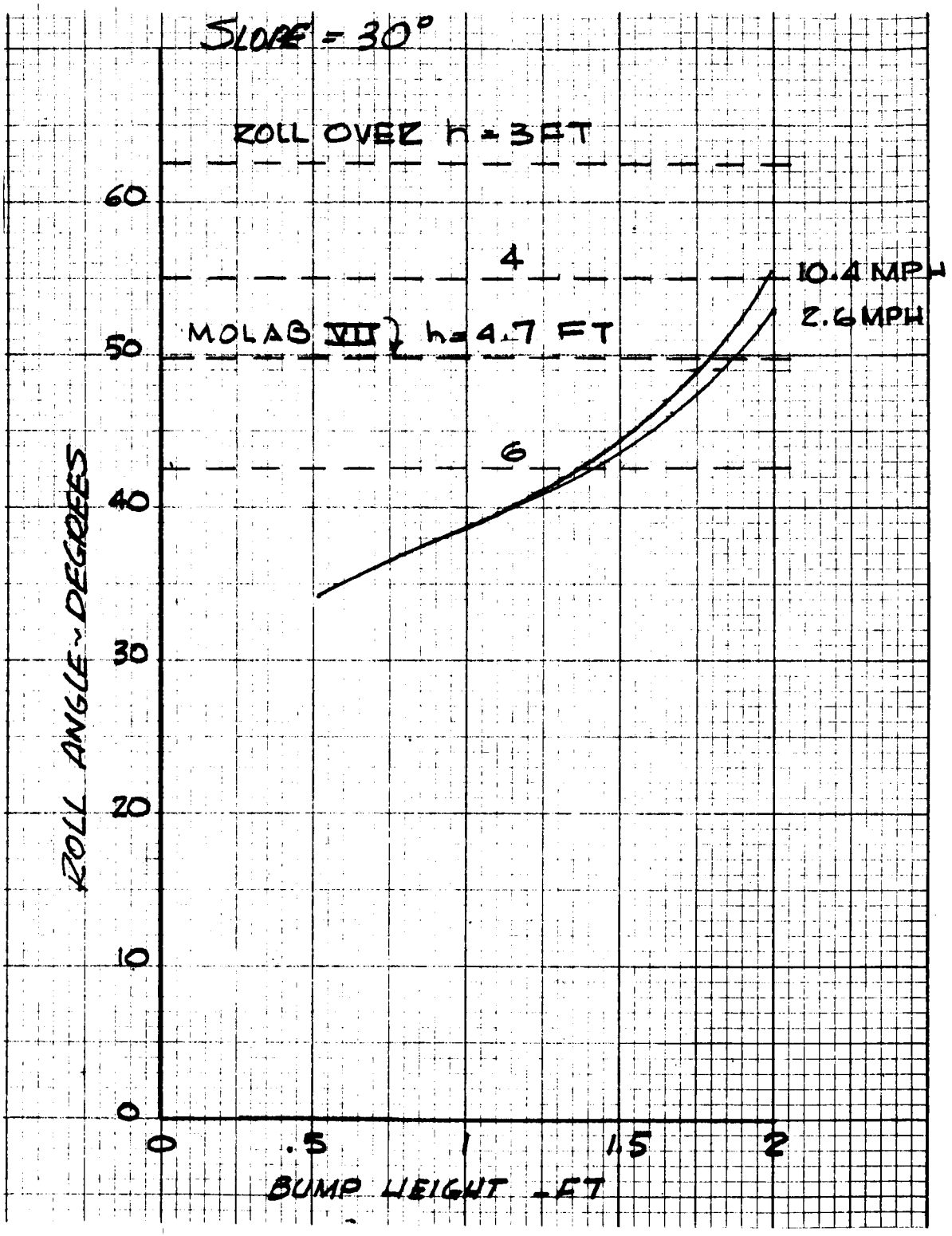

FIGURE 4D. ROLL PLANE STABILITY, SLOPE = 30°

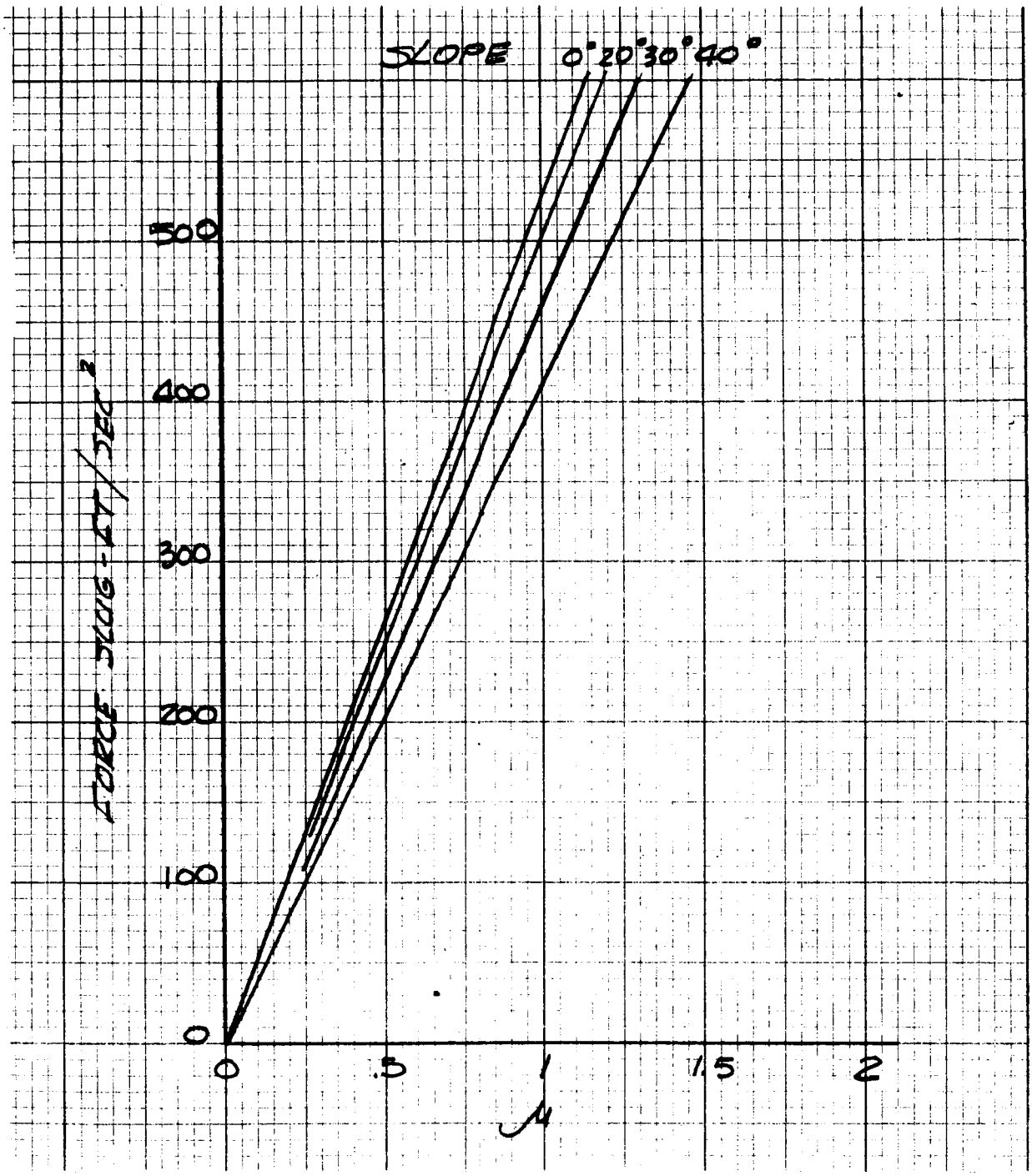

FIGURE 5. SKID POINTS - ROLL AND PITCH

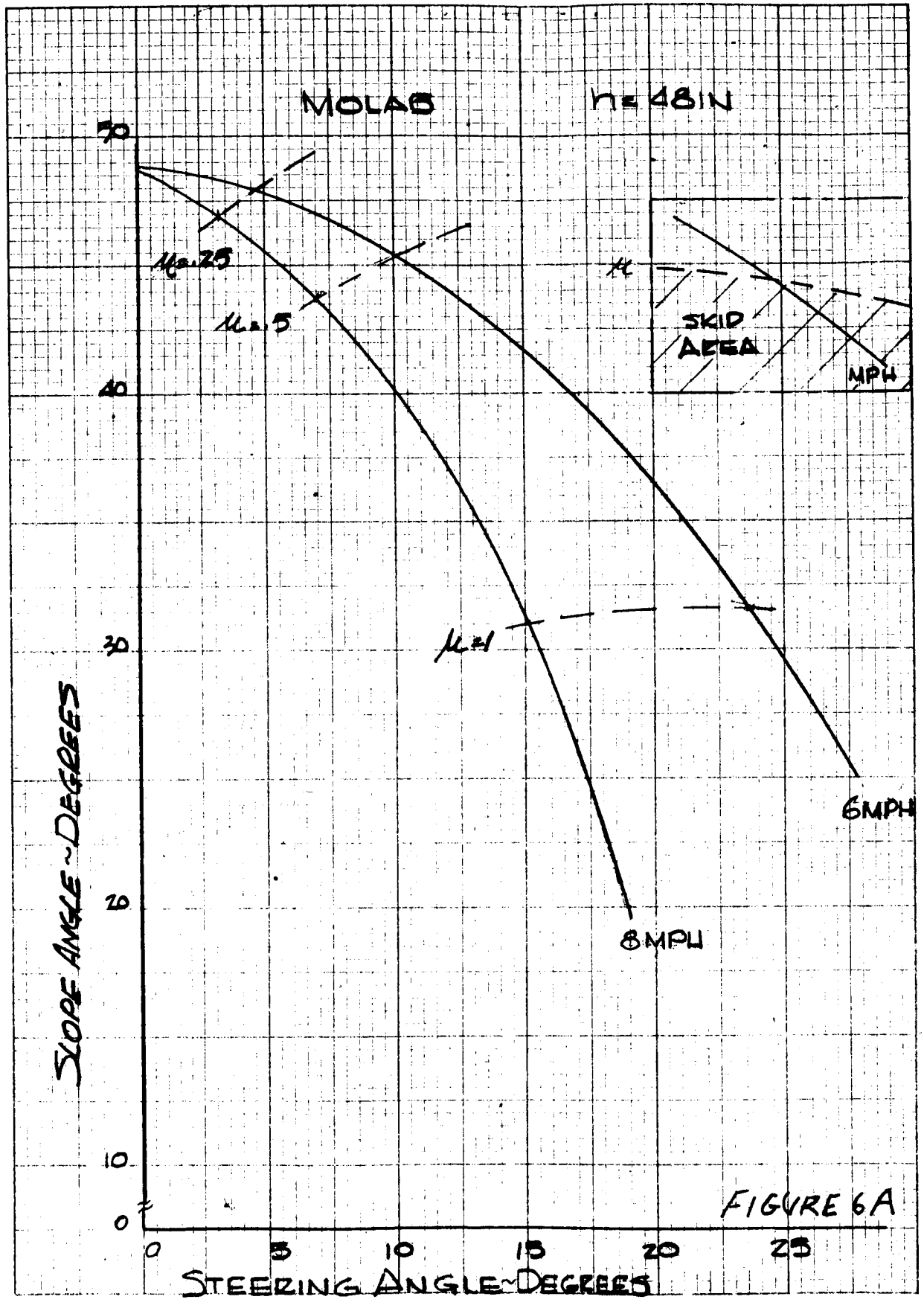

FIGURE 6A. SKID AND OVERTURN - ACKERMAN STEERING

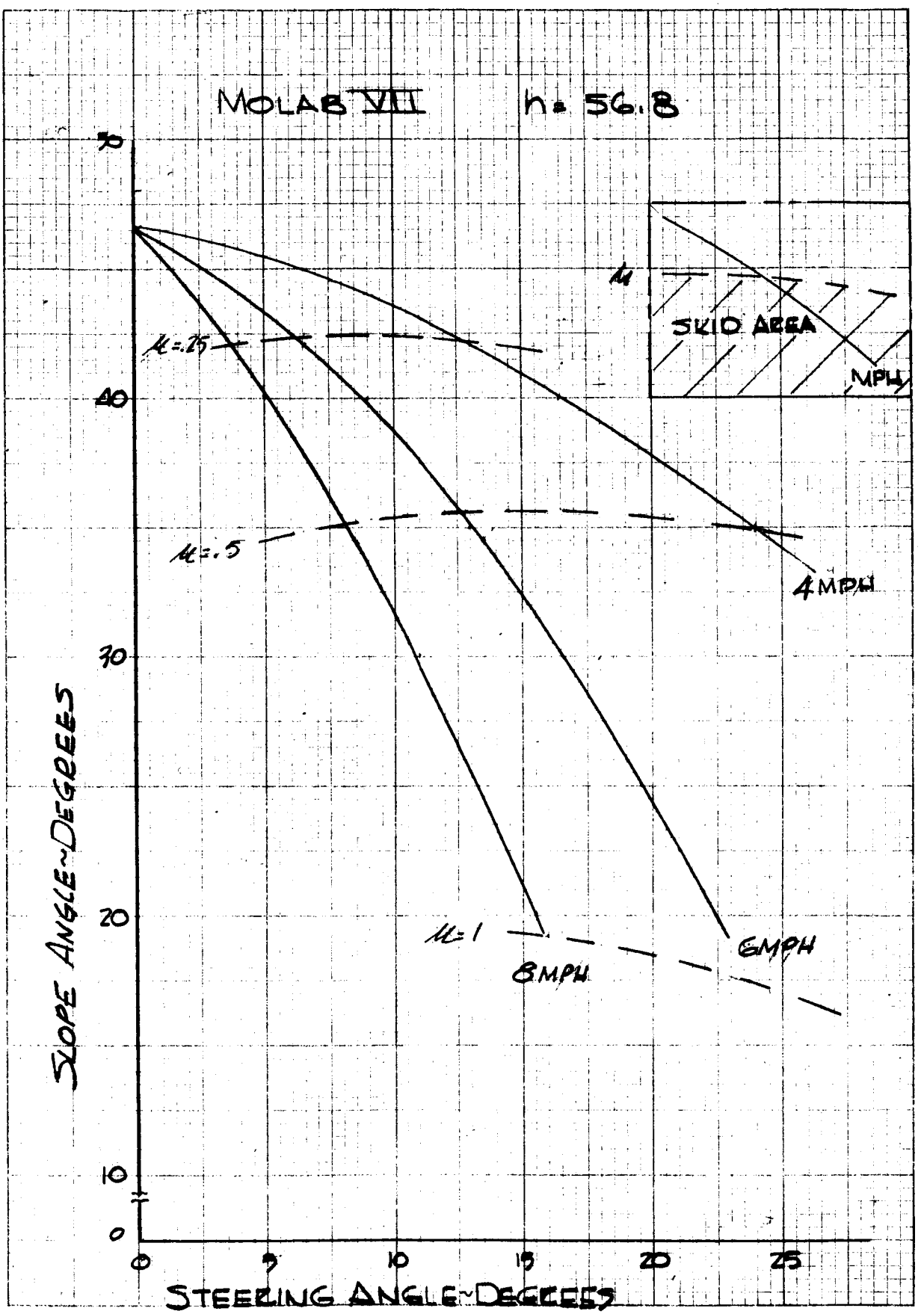

FIGURE 6B. SKID AND OVERTURN - ACKERMAN STEERING

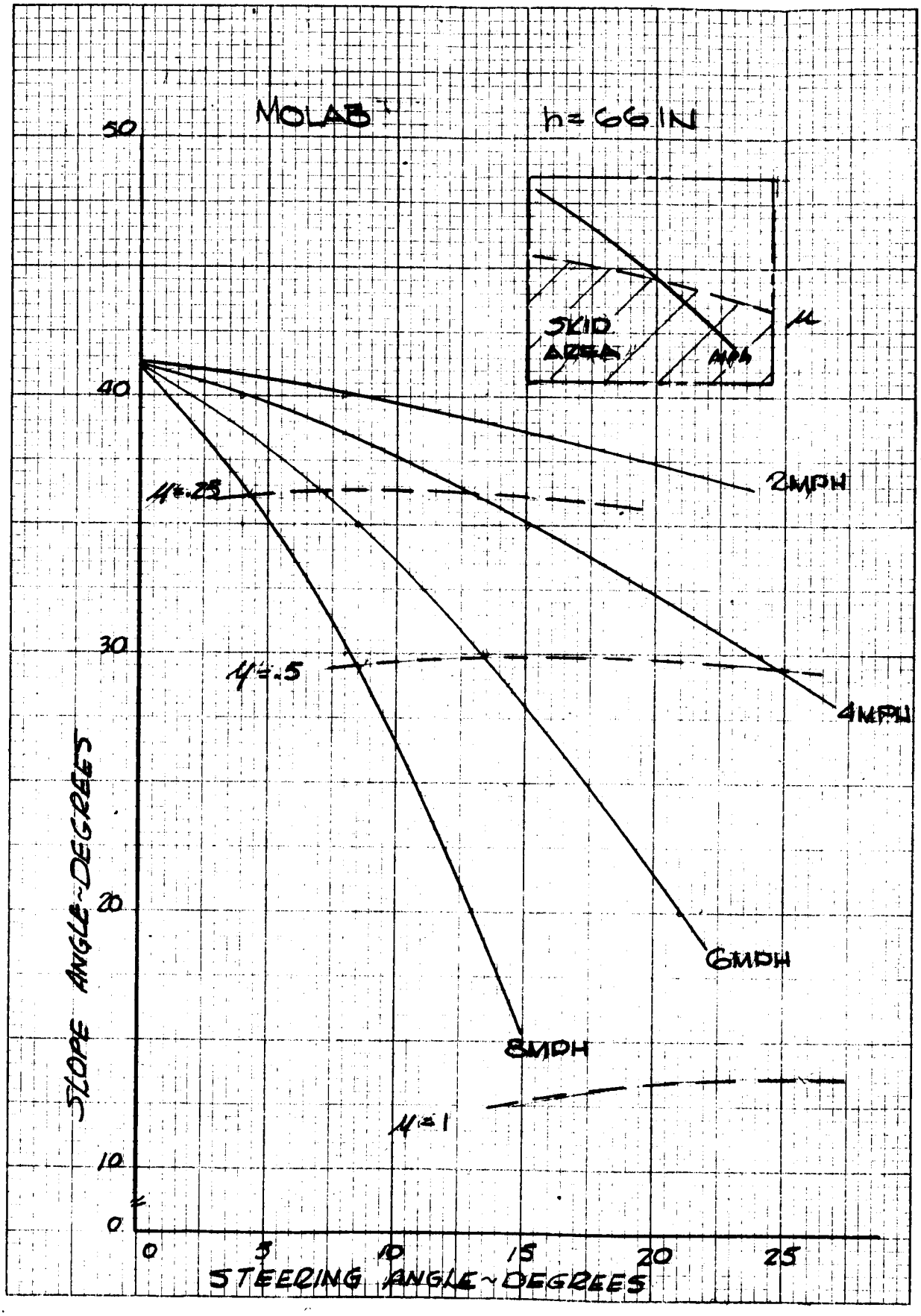

FIGURE 6C. SKID AND OVERTURN - ACKERMAN STEERING

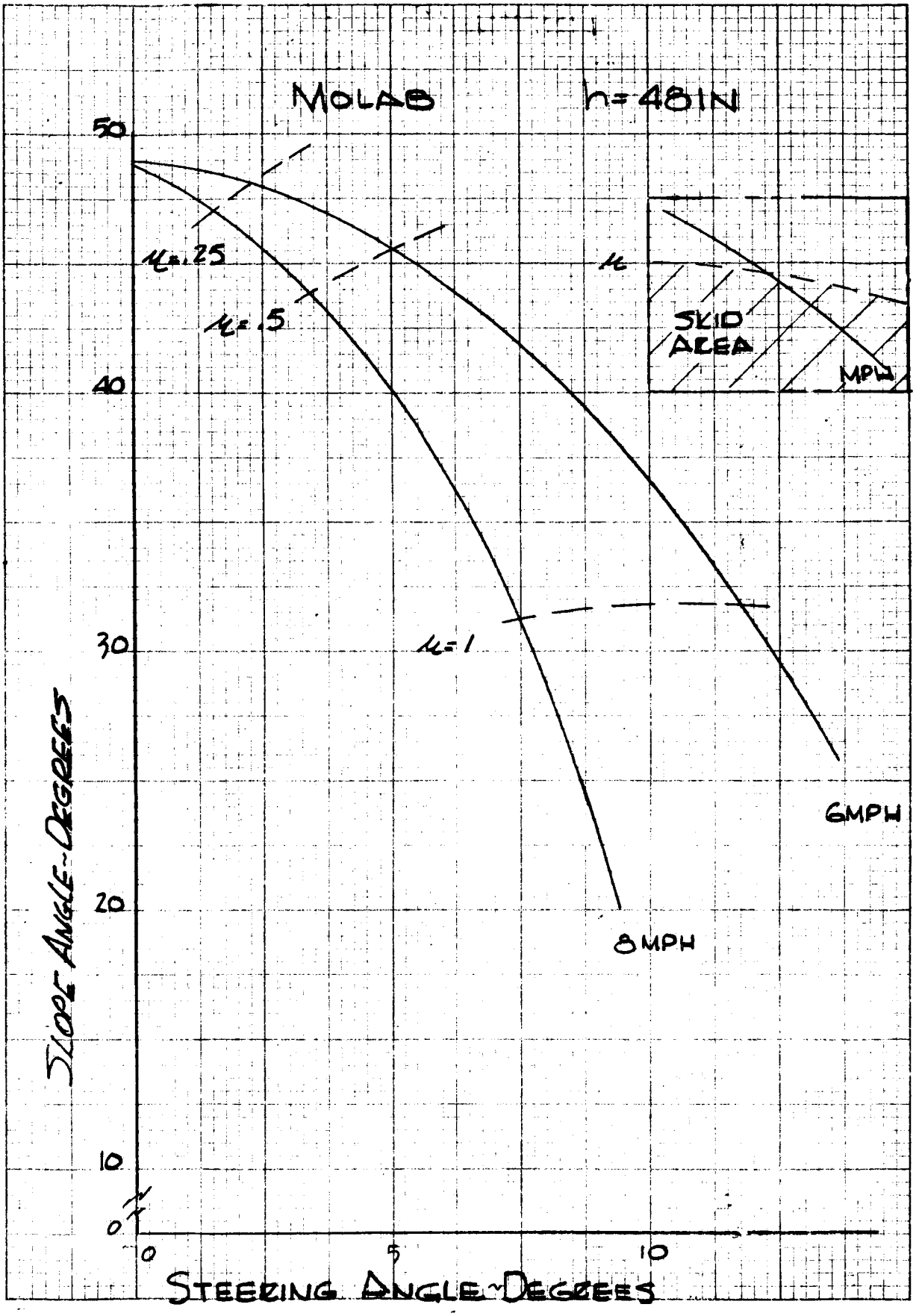

FIGURE 7A. SKID AND OVERTURN - 4 WHEEL STEERING

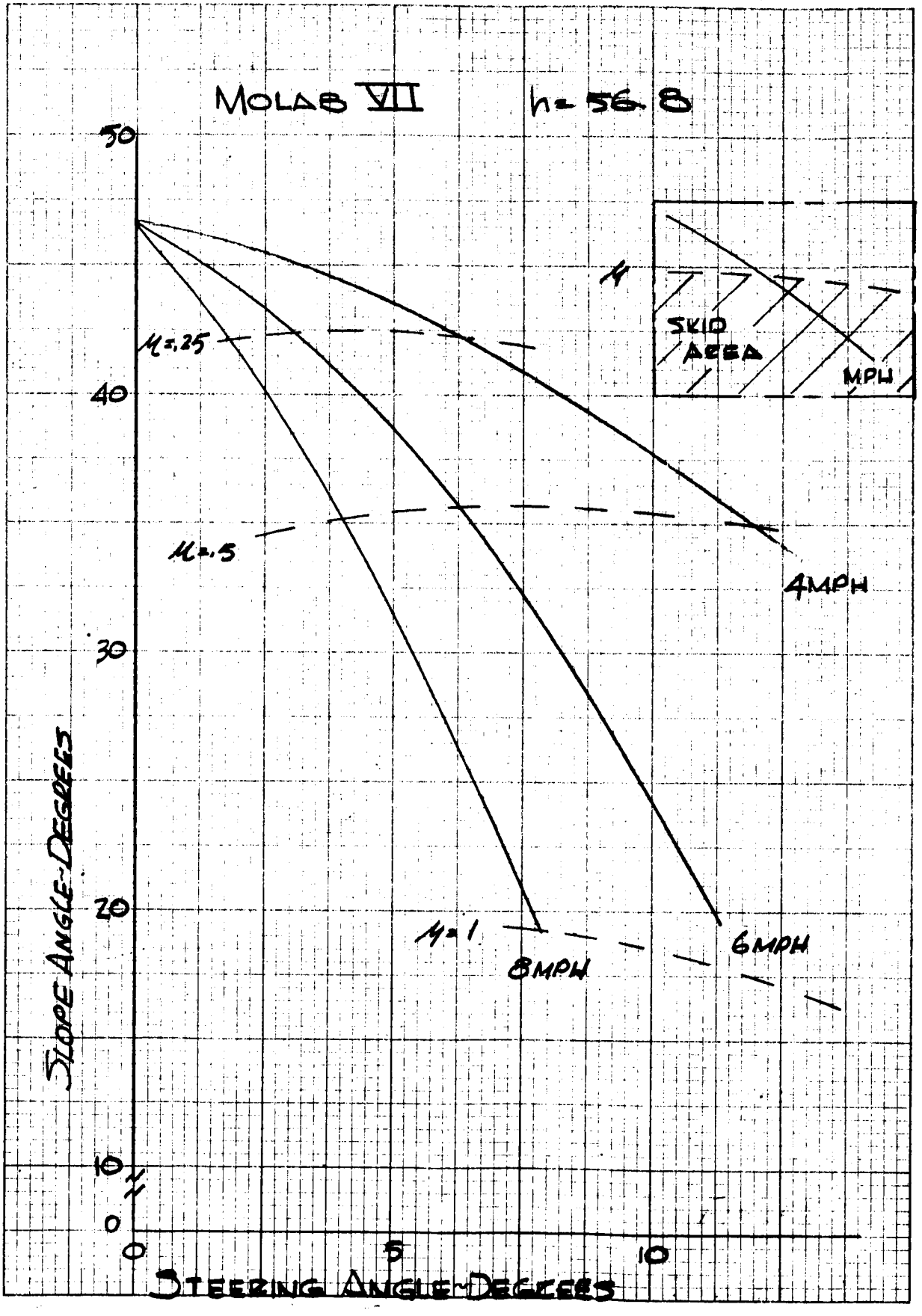

FIGURE 7B. SKID AND OVERTURN - 4 WHEEL STEERING

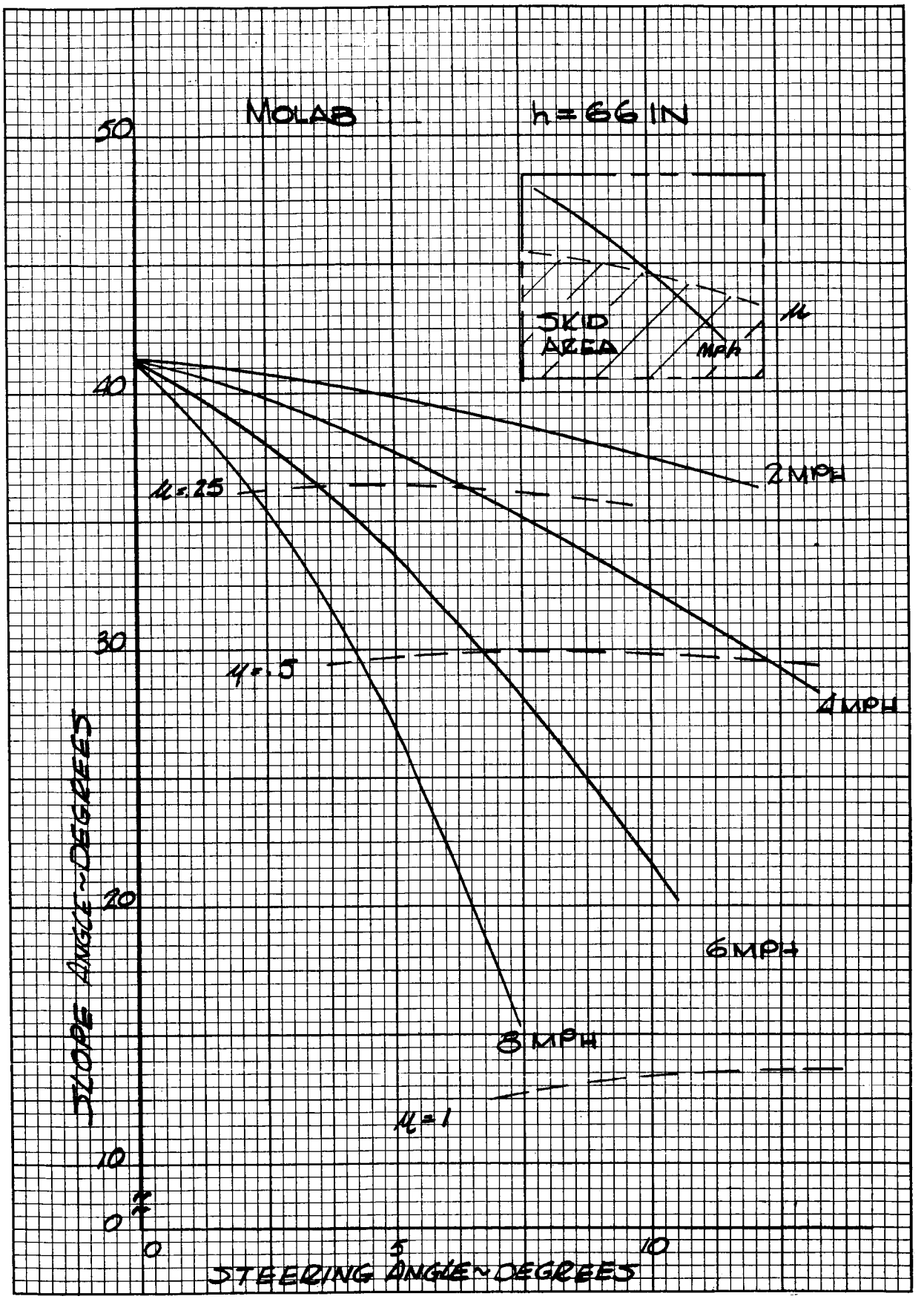

FIGURE 7C. SKID AND OVERTURN - 4 WHEEL STEERING

TABLE I

CONVERSION TABLE STEERING ANGLE TO TURNING RADIUS

FOUR WHEEL	
Steering Angle (degrees)	Turning Radius (feet)
6	37.74
10	22.11
12	18.47
16	13.93
20	11.23
22	10.25
28	8.18
ACKERMAN	
6	73.37
10	44.06
12	36.74
16	27.59
20	22.11
22	20.12
28	16.36

Before control systems can be designed properly the nature of the system to be controlled must be known. In the conceptual designs for the MOLAB a four wheel vehicle has been analyzed in the previous task order, but the dynamics of an articulated vehicle have not been examined. To this end the general equations shown in this report have been developed. The equations, while developed for a six wheel, three module vehicle, can be used, with some modification, with a four wheel, two module vehicle. Spring coupling between modules has been used. However, with additional elements to the equations an articulated vehicle with a combination of spring and knuckle coupling can be examined. The plan and side views of the vehicle for which the equations were written are shown in Figure 8, the full mathematical model is shown in Figure 9 and the equations for motion in the pitch and roll planes are shown in Figure 10.

In order to simplify the equations, coupling between the pitch and roll planes has been neglected. This simplifying will not hamper the determination of "worst" conditions in the dynamics of the MOLAB since the inclusion of the coupling will reduce the effects of a perturbation. Design for the "worst" conditions will then afford a safety factor.

The appendix contains the derivation of the equations and a complete analog program with which the characteristics of the articulated MOLAB can be examined with a relatively small amount of computer equipment. While not every conceivable perturbation to the MOLAB can be examined with this computer program, the program when implemented will afford a means of determining enough of the characteristics for design.

PART II

GENERAL EQUATIONS OF MOTION FOR AN ARTICULATED MOLAB

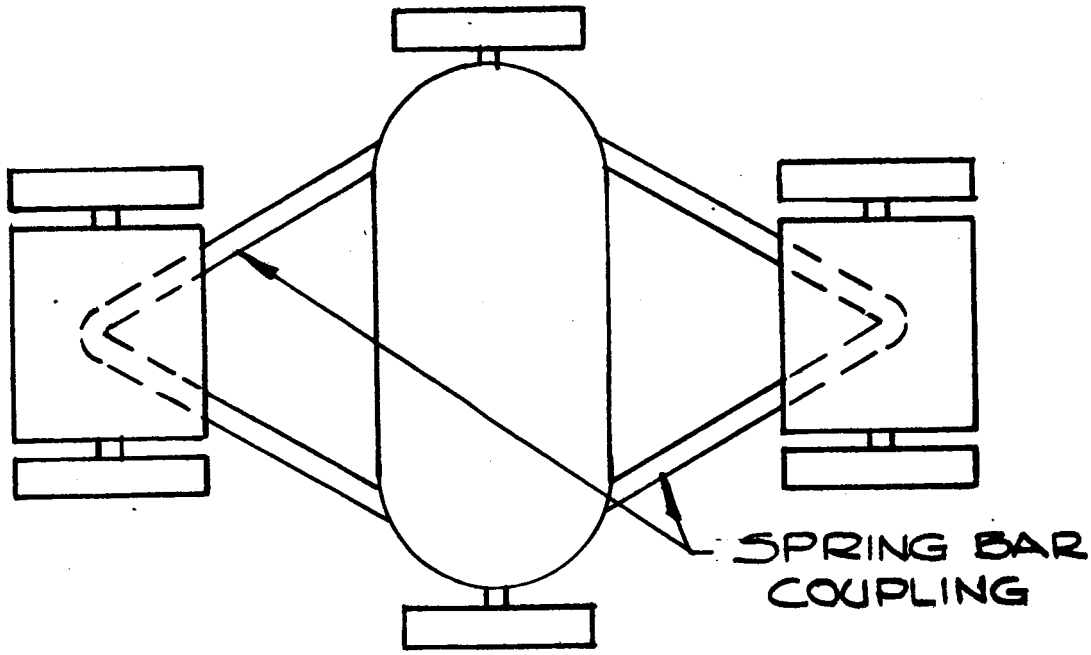

PLAN VIEW

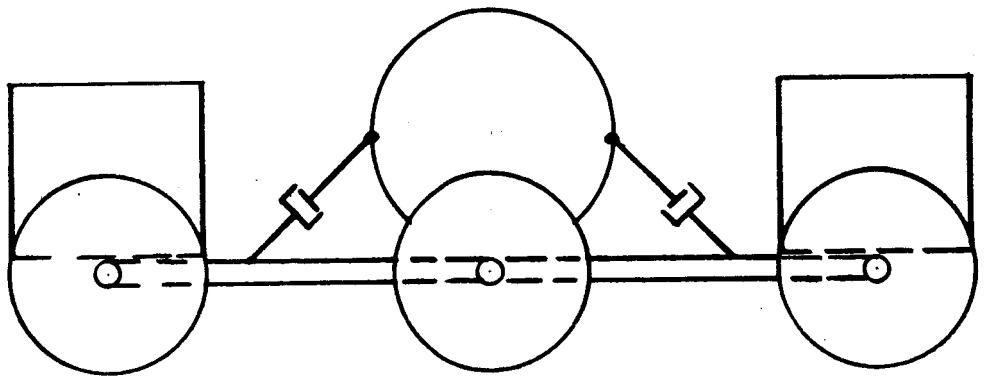

SIDE VIEW

FIGURE 8. ARTICULATED VEHICLE

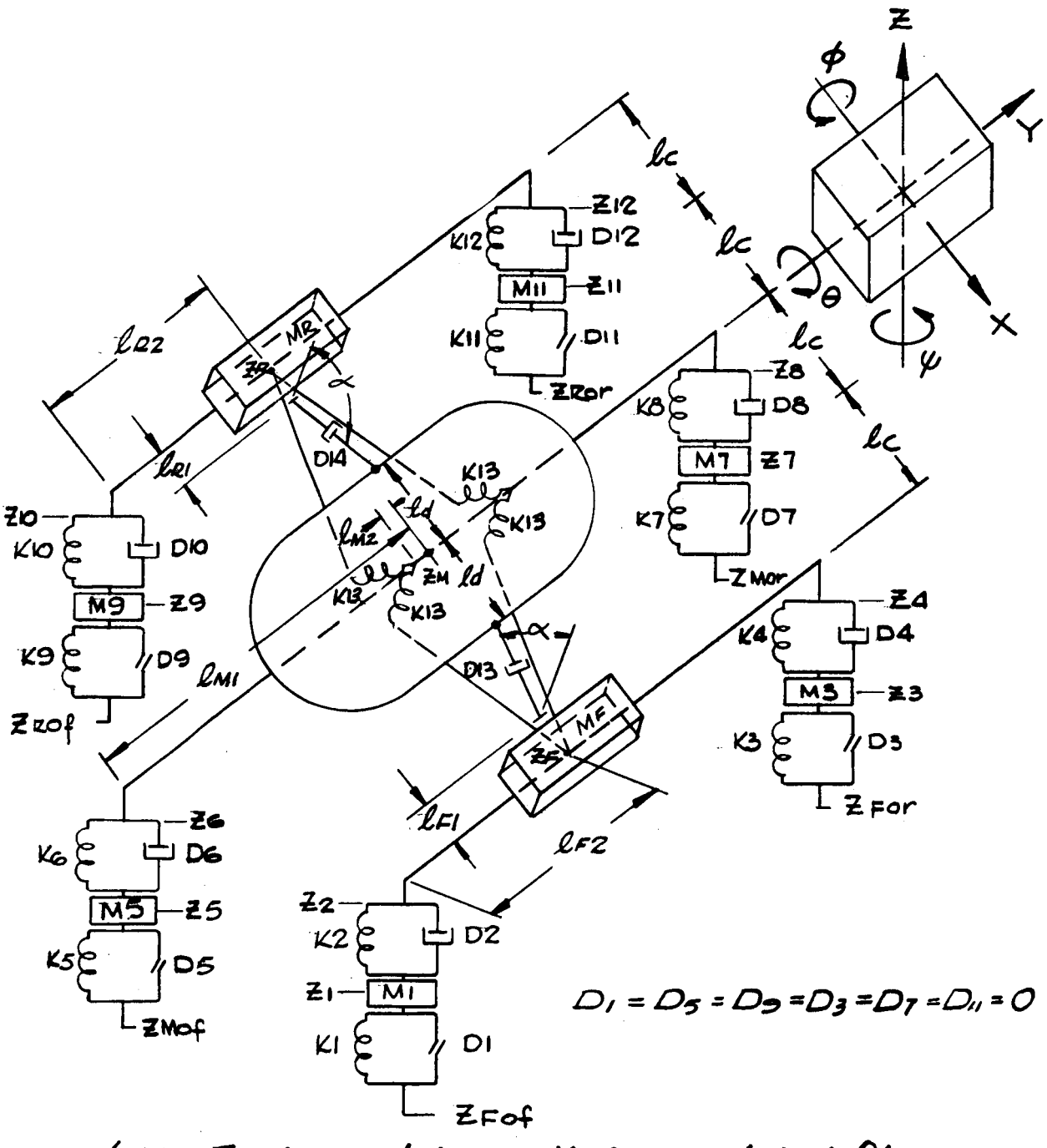

FIGURE 9. ARTICULATE MOLAB - MATHEMATICAL MODEL

FRONT MODULE
PITCH PLANE:

$$\textcircled{1}\quad -\ddot{z}_1 + \frac{K_1}{M_1}(z_{Fof} - z_1) + \frac{D_1}{M_1}(\dot{z}_{Fof} - \dot{z}_1) - \frac{K_2}{M_1}(z_1 - z_2) - \frac{D_2}{M_1}(\dot{z}_1 - \dot{z}_2) - g = 0$$

$$\textcircled{2}\quad -\ddot{z}_3 + \frac{K_3}{M_3}(z_{For} - z_3) + \frac{D_3}{M_3}(\dot{z}_{For} - \dot{z}_3) - \frac{K_4}{M_3}(z_3 - z_4) - \frac{D_4}{M_3}(\dot{z}_3 - \dot{z}_4) - g = 0$$

$$\textcircled{3}\quad -\ddot{z}_2 + \frac{2K_2}{M_F}(z_1 - z_2) + \frac{2D_2}{M_F}(\dot{z}_1 - \dot{z}_2) + \frac{2\ell_c K_{13}}{M_F}(\theta_F - \theta_M) + D_{12}C^2\frac{(\ell_c - \ell_{F1})^2}{\ell_c M_F}(\dot{\theta}_F - \dot{\theta}_M) - g = 0$$

where $C = \cos\delta$

$$\textcircled{4}\quad -\ddot{\theta}_F + \frac{2\theta_F^2 \ell_c^2 K_{13}}{I_{YF}}(\theta_F - \theta_M) - \frac{2\ell_c K_{13}}{I_{YF}}(\theta_F - \theta_M)\theta_F h = 0$$

$$\textcircled{5}\quad \ddot{z}_2 = \ddot{z}_F \qquad \ddot{z}_4 = \ddot{z}_F$$

$$\dot{z}_2 = \dot{z}_F \qquad \dot{z}_4 = \dot{z}_F$$

$$z_2 = z_F \qquad z_4 = z_F$$

FIGURE 10A. GENERAL EQUATIONS OF MOTION

MAIN MODULE
PITCH PLANE

$$\textcircled{1}\ -\ddot{z}_5 + \frac{K_5}{M_5}(z_{Mot} - z_5) + \frac{D_5}{M_5}(\dot{z}_{Mot} - \dot{z}_5) - \frac{K_6}{M_5}(z_5 - z_6)$$
$$- \frac{D_6}{M_5}(\dot{z}_5 - \dot{z}_6) - g = 0$$

$$\textcircled{2}\ -\ddot{z}_7 + \frac{K_7}{M_7}(z_{Mor} - z_7) + \frac{D_7}{M_7}(\dot{z}_{Mor} - \dot{z}_7) - \frac{K_8}{M_7}(z_7 - z_8)$$
$$- \frac{D_8}{M_7}(\dot{z}_7 - \dot{z}_8) - g = 0$$

$$\textcircled{3}\ -\ddot{z}_6 + \frac{2K_6}{M_M}(z_5 - z_6) + \frac{2D_6}{M_M}(\dot{z}_5 - \dot{z}_6) - \frac{2l_c K_{13}}{M_M}(\theta_M - \theta_F)$$
$$- \frac{2l_c K_{13}}{M_M}(\theta_R - \theta_M) - \frac{D_{13}C^2}{l_c M_M}(l_c - l_{F1})^2(\dot{\theta}_M - \dot{\theta}_F)$$
$$- \frac{D_{13}C^2}{l_c M_M}(l_c - l_{R1})^2(\dot{\theta}_R - \dot{\theta}_M) - g = 0$$

where $C = \cos\alpha$

$$\textcircled{4}\ -\ddot{\theta}_M - \frac{D_{13}l_d C}{I_{YM}}(l_c - l_{F1})(\dot{\theta}_M - \dot{\theta}_F) + \frac{D_{13}l_d C}{I_{YM}}(\dot{\theta}_R - \dot{\theta}_M)(l_c - l_{R1})$$
$$- \frac{4l_c^2 K_{13}}{I_{YM}}(\theta_M - \theta_F) + \frac{4l_c^2 K_{13}}{I_{YM}}(\theta_R - \theta_M) = 0$$

$$\textcircled{5}\quad \ddot{z}_6 = \ddot{z}_M \qquad \ddot{z}_8 = \ddot{z}_M$$
$$\dot{z}_6 = \dot{z}_M \qquad \dot{z}_8 = \dot{z}_M$$
$$z_6 = z_M \qquad z_8 = z_M$$

FIGURE 10B. GENERAL EQUATIONS OF MOTION (Cont'd)

REAR MODULE
PITCH PLANE

$$① \; -\ddot{z}_9 + \frac{K_9}{M_9}(z_{Rof} - z_9) + \frac{D_9}{M_9}(\dot{z}_{Rof} - \dot{z}_9) - \frac{K_{10}}{M_9}(z_9 - z_{10}) - \frac{D_{10}}{M_9}(\dot{z}_9 - \dot{z}_{10}) - g = 0$$

$$② \; -\ddot{z}_{11} + \frac{K_{11}}{M_{11}}(z_{Ror} - z_{11}) + \frac{D_{11}}{M_{11}}(\dot{z}_{Ror} - \dot{z}_{11}) - K_{12}(z_{11} - z_{12}) - \frac{D_{12}}{M_{11}}(\dot{z}_{11} - \dot{z}_{12}) - g = 0$$

$$③ \; -\ddot{z}_{10} + \frac{2K_{10}}{M_R}(z_9 - z_{10}) + \frac{2D_{10}}{M_R}(\dot{z}_9 - \dot{z}_{10}) - \frac{2l_c K_{13}}{M_R}(\theta_R - \theta_M) - D_{13}C^2\frac{(l_c - l_{R1})^2}{l_c M_R}(\dot{\theta}_R - \dot{\theta}_M) - g = 0$$

where $C = \cos\alpha$

$$④ \; -\ddot{\theta}_R + \frac{2\theta_R^2 l_c^2 K_{13}}{I_{YR}}(\theta_R - \theta_M) - \frac{2l_c K_{13}}{I_{YR}}(\theta_R - \theta_M)\theta_R h = 0$$

$$⑤ \quad \ddot{z}_{10} = \ddot{z}_R \qquad \ddot{z}_{12} = \ddot{z}_R$$
$$\dot{z}_{10} = \dot{z}_R \qquad \dot{z}_{12} = \dot{z}_R$$
$$z_{10} = z_R \qquad z_{12} = z_R$$

FIGURE 10C. GENERAL EQUATIONS OF MOTION (Cont'd)

FRONT MODULE
ROLL PLANE

$$\textcircled{1}\quad -\ddot{z}_1 + \frac{K_1}{M_1}(z_{Fof} - z_1) + \frac{D_1}{M_1}(\dot{z}_{Fof} - \dot{z}_1) - \frac{K_2}{M_1}(z_1 - z_2) - \frac{D_2}{M_1}(\dot{z}_1 - \dot{z}_2) - g = 0$$

$$\textcircled{2}\quad -\ddot{z}_3 + \frac{K_3}{M_3}(z_{For} - z_3) + \frac{D_3}{M_3}(\dot{z}_{For} - \dot{z}_3) - \frac{K_4}{M_3}(z_3 - z_4) - \frac{D_4}{M_3}(\dot{z}_3 - \dot{z}_4) - g = 0$$

$$\textcircled{3}\quad -\ddot{z}_F + \frac{K_2}{M_F}(z_1 - z_2) + \frac{K_4}{M_F}(z_3 - z_4) + \frac{D_2}{M_F}(\dot{z}_1 - \dot{z}_2) + \frac{D_4}{M_F}(\dot{z}_3 - \dot{z}_4) - g = 0$$

$$\textcircled{4}\quad -\ddot{\phi}_F + \frac{l_{F_2}}{I_{x_F}} K_4 (z_3 - z_4) + \frac{l_{F_2} D_4}{I_{x_F}}(\dot{z}_3 - \dot{z}_4) - \frac{l_{F_2} K_2}{I_{x_F}}(z_1 - z_2) - \frac{l_{F_2} D_2}{I_{x_F}}(\dot{z}_1 - \dot{z}_2) + \frac{2 l^2 M_2 K_{13}}{I_{x_F}}(\phi_M - \phi_F) = 0$$

$$\textcircled{5}\quad \ddot{z}_4 = \ddot{z}_F + l_{F_2}\ddot{\phi}_F \qquad \dot{z}_4 = \dot{z}_F + l_{F_2}\dot{\phi}_F \qquad z_4 = z_F + l_{F_2}\phi_F$$
$$\ddot{z}_2 = \ddot{z}_F - l_{F_2}\ddot{\phi}_F \qquad \dot{z}_2 = \dot{z}_F - l_{F_2}\dot{\phi}_F \qquad z_2 = z_F - l_{F_2}\phi_F$$

FIGURE 10D. GENERAL EQUATIONS OF MOTION (Cont'd)

MAIN MODULE

ROLL PLANE

$$\textcircled{1}\ -\ddot{z}_5 + \frac{K_5}{M_5}(z_{Mot} - z_5) + \frac{D_5}{M_5}(\dot{z}_{Mot} - \dot{z}_5) - \frac{K_6}{M_5}(z_5 - z_6)$$
$$- \frac{D_6}{M_5}(\dot{z}_5 - \dot{z}_6) - g = 0$$

$$\textcircled{2}\ -\ddot{z}_7 + \frac{K_7}{M_7}(z_{Mor} - z_7) + \frac{D_7}{M_7}(\dot{z}_{Mor} - \dot{z}_7) - \frac{K_8}{M_7}(z_7 - z_8)$$
$$- \frac{D_8}{M_1}(\dot{z}_7 - \dot{z}_8) - g = 0$$

$$\textcircled{3}\ -\ddot{z}_M + \frac{K_8}{M_M}(z_7 - z_8) + \frac{D_8}{M_M}(\dot{z}_7 - \dot{z}_8) + \frac{K_5}{M_M}(z_5 - z_6) + \frac{D_6}{M_M}(\dot{z}_5 - \dot{z}_6)$$
$$- g = 0$$

$$\textcircled{4}\ -\ddot{\phi}_M + \frac{l_{M1}}{I_{x_M}} K_8 (z_7 - z_8) + \frac{l_{M1}}{I_{x_M}} D_8 (\dot{z}_1 - \dot{z}_8) - \frac{l_{M1}}{I_{x_M}} K_6 (z_5 - z_6)$$
$$- \frac{l_{M1}}{I_{x_M}} D_6 (\dot{z}_5 - \dot{z}_6) - \frac{2 l^2_{M2} K_{13}}{I_{x_M}} (\phi_M - \phi_R) - \frac{2 l^2_{M2} K_{13}}{I_{x_M}} (\phi_M - \phi_R) = 0$$

$$\textcircled{5}\ \ddot{z}_6 = \ddot{z}_M - l_{M1}\ddot{\phi}_M \qquad \dot{z}_6 = \dot{z}_M - l_{M1}\dot{\phi}_M \qquad z_6 = z_M - l_{M1}\phi_M$$
$$\ddot{z}_8 = \ddot{z}_M + l_{M1}\ddot{\phi}_M \qquad \dot{z}_8 = \dot{z}_M + l_{M1}\dot{\phi}_M \qquad z_8 = z_M - l_{M1}\phi_M$$

FIGURE 10E. GENERAL EQUATIONS OF MOTION (Cont'd)

REAR MODULE

ROLL PLANE

$$① -\ddot{z}_9 + \frac{K_9}{M_9}(z_{Rot} - z_9) + \frac{D_9}{M_9}(\dot{z}_{Rot} - \dot{z}_9) - \frac{K_{10}}{M_9}(z_9 - z_{10})$$
$$- \frac{D_{10}}{M_9}(\dot{z}_9 - \dot{z}_{10}) - g = 0$$

$$② -\ddot{z}_{11} + \frac{K_{11}}{M_{11}}(z_{Ror} - z_{11}) + \frac{D_{11}}{M_{11}}(\dot{z}_{Ror} - \dot{z}_{11}) - \frac{K_{12}}{M_{11}}(z_{11} - z_{12})$$
$$- \frac{D_{12}}{M_{11}}(\dot{z}_{11} - \dot{z}_{12}) - g = 0$$

$$③ -\ddot{z}_R + \frac{K_{10}}{M_R}(z_9 - z_{10}) + \frac{D_{10}}{M_R}(\dot{z}_9 - \dot{z}_{10}) + \frac{K_{12}}{M_R}(z_{11} - z_{12}) + \frac{D_{12}}{M_R}(\dot{z}_{11} - \dot{z}_{12}) -$$
$$- g = 0$$

$$④ -\ddot{\phi}_R + \frac{l_{R_2}}{I_{x_R}} K_{12}(z_{11} - z_{12}) + \frac{l_{R_2}}{I_{x_R}} D_{12}(\dot{z}_{11} - \dot{z}_{12}) - \frac{l_{R_2}}{I_{x_R}} K_{10}(z_9 - z_{10})$$
$$- \frac{l_{R_2}}{I_{x_R}} D_{10}(\dot{z}_9 - \dot{z}_{10}) + \frac{2 l_{M_2}^2 K_{13}}{I_{x_R}}(\phi_M - \phi_R) = 0$$

$$⑤ \ddot{z}_{12} = \ddot{z}_R + l_{R_2}\ddot{\phi}_R \quad \dot{z}_{12} = \dot{z}_R + l_{R_2}\dot{\phi}_R \quad z_{12} = z_R + l_{R_2}\phi_R$$
$$\ddot{z}_{10} = \ddot{z}_R - l_{R_2}\ddot{\phi}_R \quad \dot{z}_{10} = \dot{z}_R - l_{R_2}\dot{\phi}_R \quad z_{10} = z_R - l_{R_2}\phi_R$$

FIGURE 10F. GENERAL EQUATIONS OF MOTION (Cont'd)

SECTION 3.0

SYMBOLS

CG	Center of gravity.
D( )	Damping constant, lb/ft/sec.
h	Height of CG, ft.
I_x	Moment of inertia about x axis (roll plane), slug-ft^2
I_y	Moment of inertia about y axis (pitch plane), slug-ft^2
K( )	Spring constant, lb/ft.
l( )	Moment arm, ft.
M( )	Mass, slugs.
r	Turning radius, ft.
$\ddot{Z}$( )	Vertical displacement, ft.
Θ( )	Angular position in pitch plane, radians.
Φ( )	Angular position in roll plane, radians.
ψ	Angular position in yaw plane, radians.
α	Angle between vertical, with vehicle at rest, and line of attachment of damping between modules, radians.
F	Front
F_1	Distance from point of connection of front module to module coupling arm and point of attachment of damping.
F_2	Lever arm from center of front module to center of front module wheel.
M	Main

M1	Lever arm from center of main module to center of main module wheel.
M2	Lever arm from center of main module to point at wheel module couplings are attached.
of	Bottom of wheels, right side of vehicle.
or	Bottom of wheel, left side of vehicle.
R	Rear
R1	Distance from point of connection of rear module to module coupling and point of attachment of damping.
R2	Lever arm from center of rear module to center of rear module wheel.

DERIVATION OF EQUATIONS

PITCH PLANE

Figure A-11shows equations derived for the analog computer program. It can be noted that equations for the left wheels, which were shown in the general equations are not included here. This program is developed for a six-wheel articulated vehicle where the right and left wheels of a module receive the same initial input distrubance. As such the vehicle can be examined for perturbations affecting a single module, but not a single wheel. It is felt, however, that examinination of the vehicle using continous frequency and step functions in the pitch plane on all or seperate modules and examination of single wheel disturbances in the roll plane plane (To be described later) will furnish data describing the vehicle performance.

Front, rear and main module wheel equations were developed from simple theory of motion for bodies connected by two springs and should require no further explanation. It should be noted, however, that for this computer program the structural damping of the tire has been neglected.

Since the equations of motion for the three bodies are spring-coupled together as part of the structure, an explanation of the derivation of the equations follows. Small angle theory is used through out. Figure A-11B shows the means of deriving the coupling equations for displacement and rotation between the front and main modules. K_{13}, shown in the diagrams with a spring symbol, is a distributed spring constant for each of the leaf springs (four total) connecting the modules. The fourth element of the front module displacement equation is derived by multiplying the displacement of the front module-relation to main module (calculated using small angle theory as shown) by twice the constant K_{13}. The fifth element is derived by calculating the vertical contribution of the damping between the modules and transporting its effect under the center of gravity by multiplying it by $\frac{l_c - l_f}{l_c}$. Since the force on the front body is in the down direction and the angle generated is negative, both elements are preceded by a plus sign.

The second and third elements of the front module rotation equation were generated as shown on Figure A-11Bby taking moments about the center of gravity. Forces other than those contributed by the coupling spring were negelected. Again the mathematical signs of the elements were dtermined by the fact that the angle shown is negative.

Displacement and rotation equations for the rear module were generated in a manner similar as those for the front module with appropriate sign changes caused by having a positive pitch angle on

the rear module.

The equations for the main module are those of the front and rear module with the signs reversed. There is one exception in the equations of rotation. Since the damping arm is considered to be stiff, the vertical contribution of damping to the rotation of the main body is transported from the point of attachment to the coupling to the point of attachment to the main body and the lever arm, l_d is used.

ROLL PLANE

The equations of motion for the roll plane for a six wheel vehicle were developed as shown in Figures A-11C, A-11D, A-11E. The displacement equations for the wheels and bodies of the three modules were derived using simple theory for masses coupled by two springs. It can be noted, however, that the structural damping for the tires is neglected.

Coupling equations between displacement and rotation are also of a standard form.

In developing equations for rotation small angle theory was used. The equations for the torque coupling between any two modules represent the relative rotation between the two bodies. The difference in rotation, represented by $l_{m2}(\phi_m - \phi_m - \phi_{f,r})$, when multiplied by the spring constant K_{13} and the lever arm (about the center of gravity) l_{m2} gives the desired angular forces. Other elements of the rotation equation are of a standard form.

ANALOG COMPUTER MODEL

This analog computer model was developed for a six wheel vehicle, and the scaling applies for parameters of the following order.

$\ddot{Z} = 50' / sec^2$	$\ddot{\Theta} = 2$ Rad/sec^2	$\ddot{\phi} = 2$ Rad/sec^2
$\dot{Z} = 20' / sec$	$\dot{\Theta} = 2$ Rad/sec	$\dot{\phi} = 2$ Rad/sec
$Z = 20'$	$\Theta = 2$ Rad	$\phi = 2$ Rad

$l_c = 5.1'$	$C = 0.707$
$l_{F1} = 2.7' = l_{R1}$	$M_m = 74$
$l_{F2} = 2.9' = l_{R2}$	$M_1 = 1.86 = M_5 = M_9 = M_3 = M_7 = M_{11}$
$l_{m1} = 6.7'$	$M_F = 58.5 = M_R$
$l_{m2} = 3.4'$	$I_{yf} = 157.4 = I_{yr}$
$l_d = 3.1'$	$I_{ym} = 383$

SECTION 4.0

APPENDIX

SUBSCRIPTS

1. Right wheel front module.
2. Right chassis front module.
3. Left wheel, front module.
4. Left chassis, front module.
5. Right wheel main module.
6. Right chassis main module.
7. Left wheel main module.
8. Left chassis main module.
9. Right wheel rear module.
10. Right chassis rear module.
11. Left wheel rear module.
12. Left chassis rear module.
13. Coupling between modules.

c. Half the length of coupling between modules.

d. Distance from center of main module to point at which damping between modules is attached.

$$I_{xf} = 154 = I_{xr}$$

$$I_{xm} = 905$$

$D_1=O=D_5=D_7=D_3=D_{11}$

$D_2=D_4=100, \quad 250 = D_{10}=D_{12}$

$D_6=D_8=150, \quad 350$

$K_1=K_3=500, \quad 900=K_9=K_{11}=K_{10}=K_{12}=K_5=K_7$

$K_6=K_8=600, \quad 1400$

$K_{13}=500, \quad 1500$

$D_{13}=250, \quad 750$

Note that in the equations of rotation of the main module in the roll plane the front and rear module torque effects are combined into one element. Computer diagrams are shown in Figure A-12.

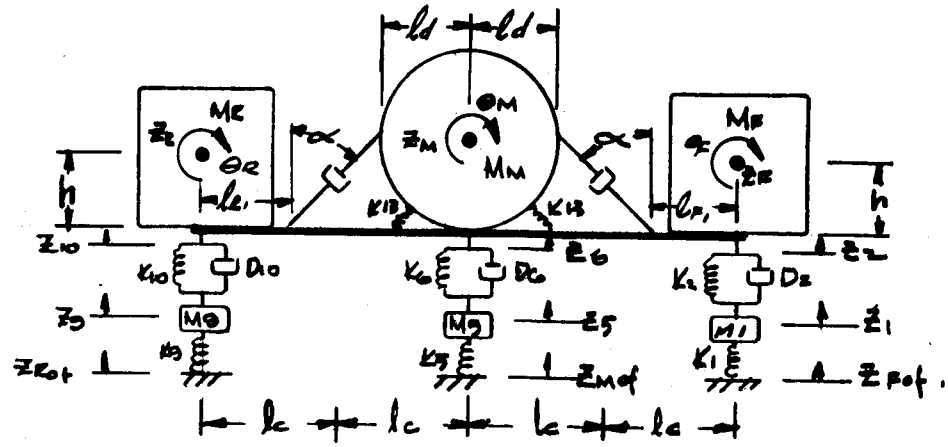

EQUATIONS

FRONT WHEEL

$$-\ddot{z}_1+\frac{K_1'}{M_1}(z_{Fof}-z_1)-\frac{D_2'}{M_1}(\dot{z}_{Fof}-\dot{z}_1)-\frac{K_2'}{M_1}(z_1-z_2)-g=0$$

REAR WHEEL

$$-\ddot{z}_9+\frac{K_9}{M_9}(z_{Rof}-z_9)-\frac{D_{10}}{M_9}(\dot{z}_9-\dot{z}_{10})-\frac{K_{10}}{M_9}(z_9-z_{10})-g=0$$

MAIN WHEEL

$$-\ddot{z}_5+\frac{K_5}{M_5}(z_{Mof}-z_5)-\frac{D_6}{M_5}(\dot{z}_{Mof}-\dot{z}_5)-\frac{K_6}{M_5}(z_5-z_6)-g=0$$

FRONT BODY - DISPLACEMENT

$$-\ddot{z}_2+\frac{2K_2}{M_F}(z_1-z_2)+\frac{2D_2}{M_F}(\dot{z}_1-\dot{z}_2)+\frac{2l_cK_{13}}{M_F}(\theta_F-\theta_M)+\frac{D_{13}C^2(l_c-l_F)^2}{l_cM_F}(\theta_F-\theta_M)+g=0$$

$\ddot{z}_F=\ddot{z}_2$; $\dot{z}_F=\dot{z}_2$; $z_F=z_2$

FRONT BODY - ROTATION

$$-\ddot{\theta}_F+\frac{2\theta_F^2l_c^2K_{13}}{I_{YF}}(\theta_F-\theta_M)-\frac{2l_cK_{13}\theta_Fh}{I_{YF}}(\theta_F-\theta_M)=0$$

REAR BODY - DISPLACEMENT

$$-\ddot{z}_{10}+\frac{2K_{10}}{M_E}(z_9-z_{10})+\frac{2D_{10}}{M_E}(\dot{z}_9-\dot{z}_{10})-\frac{2l_cK_{13}}{M_E}(\theta_E-\theta_M)-\frac{D_{13}C^2(l_c-l_F)^2}{l_cM_F}(\dot{\theta}_E-\dot{\theta}_M)-g=0$$

$\ddot{z}_E=\ddot{z}_{10}$; $\dot{z}_E=\dot{z}_{10}$; $z_E=z_{10}$

REAR BODY - ROTATION

$$-\ddot{\theta}_E+\frac{2\theta_E^2l_c^2K_{13}}{I_{YE}}(\theta_E-\theta_M)-\frac{2l_cK_{13}\theta_Eh}{I_{YE}}(\theta_E-\theta_M)=0$$

MAIN BODY - DISPLACEMENT

$$-\ddot{z}_6+\frac{2K_6}{M_M}(K_5-K_6)+\frac{2D_6}{M_M}(\dot{z}_5-\dot{z}_6)-\frac{2l_cK_{13}}{M_M}(\theta_M-\theta_F)-\frac{2l_cK_{13}}{M_M}(\theta_E-\theta_M)$$

$$-\frac{D_{13}C^2}{M_M}(l_c-l_F)^2(\dot{\theta}_M-\dot{\theta}_F)-\frac{D_{13}C^2}{l_cM_M}(l_c-l_{E1})^2(\dot{\theta}_E-\dot{\theta}_M)-g=0\ ;\ \ddot{z}_M=\ddot{z}_6\ ;\ \dot{z}_M=\dot{z}_6\ ;\ z_M=z_6$$

MAIN BODY - ROTATION

$$-\ddot{\theta}_M-\frac{D_{13}l_dC}{I_{YM}}(l_c-l_F)(\dot{\theta}_M-\dot{\theta}_F)+\frac{D_{13}l_dC}{I_{YM}}(l_c-l_{E1})(\dot{\theta}_E-\dot{\theta}_M)-\frac{4l_c^2K_{13}}{I_{YM}}(\theta_M-\theta_F)$$

$$+\frac{4l_c^2K_{13}}{I_{YM}}(\theta_E-\theta_M)=0$$

FIGURE A11A. DERIVATION OF EQUATIONS - PITCH PLANE

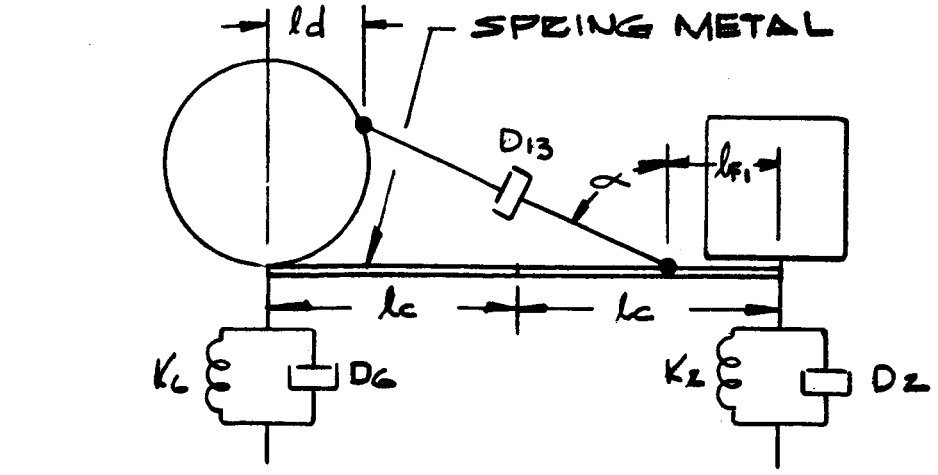

MAIN AND FRONT MODULES AT REST

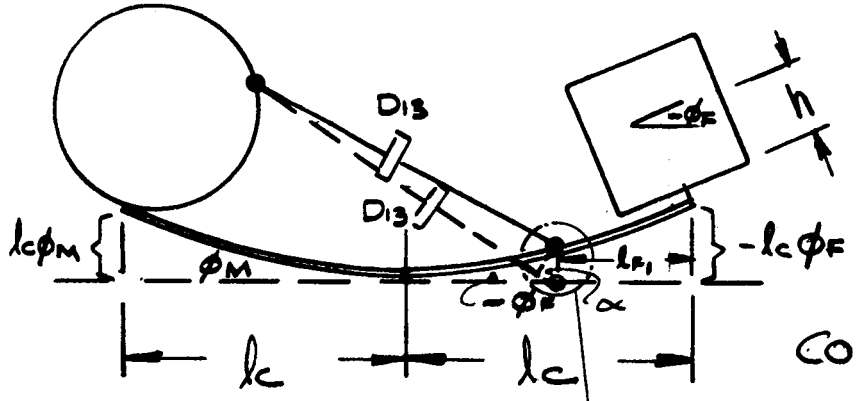

MAIN AND FRONT MODULES DISTURBED

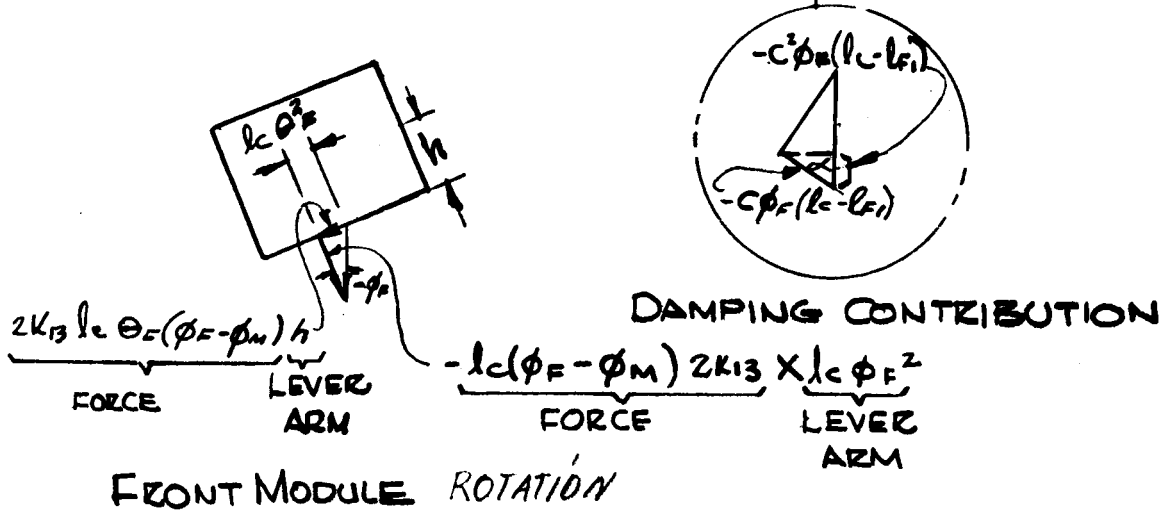

FIGURE A11B. DERIVATION OF EQUATIONS - FRONT AND MAIN MODULES

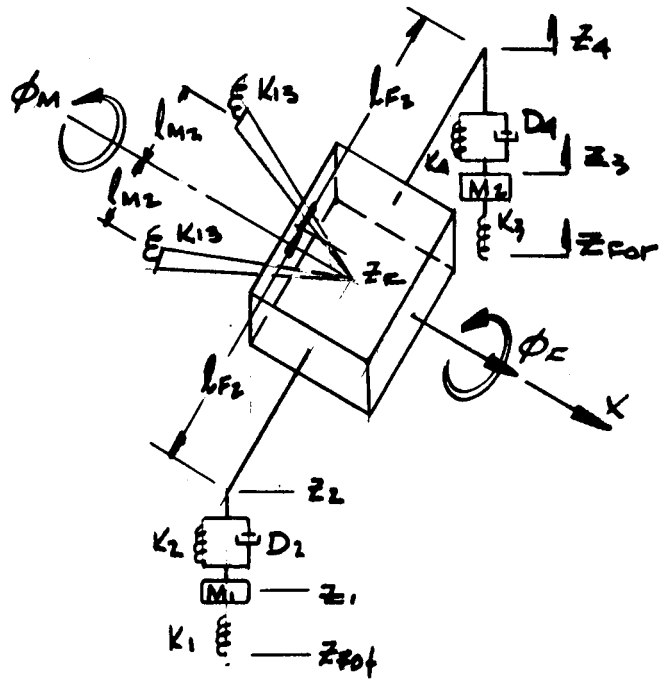

WHEEL EQUATIONS

$$-\ddot{z}_1 + \frac{K_1}{M_1}(z_{Fof} - z_1) + \frac{D_1}{M_1}(\dot{z}_{Fof} - \dot{z}_1) - \frac{K_2}{M_1}(z_1 - z_2) - \frac{D_2}{M_1}(\dot{z}_1 - \dot{z}_2) - g = 0$$

$$-\ddot{z}_3 + \frac{K_3}{M_3}(z_{For} - z_3) + \frac{D_3}{M_3}(\dot{z}_{For} - \dot{z}_3) - \frac{K_4}{M_3}(z_3 - z_4) - \frac{D_4}{M_3}(\dot{z}_3 - \dot{z}_4) - g = 0$$

BODY EQUATION - DISPLACEMENT

$$-\ddot{z}_F + \frac{K_2}{M_F}(z_1 - z_2) + \frac{K_4}{M_F}(z_3 - z_4) + \frac{D_2}{M_F}(\dot{z}_1 - \dot{z}_2) + \frac{D_4}{M_F}(\dot{z}_3 - \dot{z}_4) - g = 0$$

BODY EQUATION - ROTATION

$$-\ddot{\Theta}_F + \frac{l_{F2}}{I_{YF}} K_4 (z_3 - z_4) + \frac{l_{F2} D_4}{I_{YF}} (\dot{z}_3 - \dot{z}_4) - \frac{l_{F2} K_2}{I_{YF}} (z_1 - z_2) - \frac{l_{F2} D_2}{I_{YF}} (\dot{z}_1 - \dot{z}_2)$$

$$+ \frac{2 l^2_{M2} K_{13}}{I_{XF}} (\phi_M - \phi_F) = 0$$

COUPLING EQUATIONS

$$\ddot{z}_4 = \ddot{z}_F + l_{F2}\ddot{\phi}_F \qquad \dot{z}_4 = \dot{z}_F + l_{F2}\dot{\phi}_F \qquad z_4 = z_F + l_{F2}\phi_F$$

$$\ddot{z}_2 = \ddot{z}_F - l_{F2}\ddot{\phi}_F \qquad \dot{z}_2 = \dot{z}_F - l_{F2}\dot{\phi}_F \qquad z_2 = z_F - l_{F2}\phi_F$$

FIGURE A11C. DERIVATION OF EQUATIONS - ROLL PLANE (FRONT MODULE)

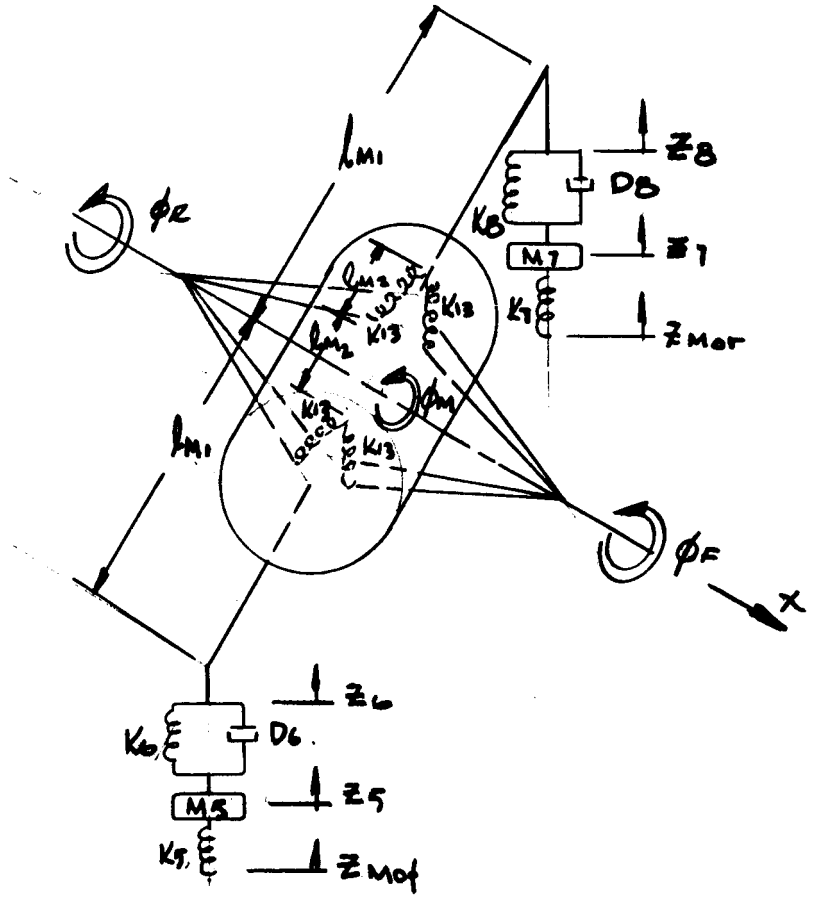

WHEEL EQUATIONS

$$-\ddot{z}_5+\frac{K_5}{M_5}(z_{mof}-z_5)+\frac{D_5}{M_5}(\dot{z}_{mof}-\dot{z}_5)-\frac{K_6}{M_5}(z_5-z_6)-\frac{D_6}{M_5}(\dot{z}_5-\dot{z}_6)-g=0$$

$$-\ddot{z}_7+\frac{K_7}{M_7}(z_{mor}-z_7)+\frac{D_7}{M_7}(\dot{z}_{mor}-\dot{z}_7)-\frac{K_8}{M_7}(z_7-z_8)-\frac{D_8}{M_7}(\dot{z}_7-\dot{z}_8)-g=0$$

BODY EQUATION - DISPLACEMENT

$$-\ddot{z}_M+\frac{K_8}{M_M}(z_7-z_8)+\frac{D_8}{M_M}(\dot{z}_7-\dot{z}_8)+\frac{K_6}{M_M}(z_5-z_6)+\frac{D_6}{M_M}(\dot{z}_5-\dot{z}_6)+g=0$$

BODY EQUATION - ROTATION

$$-\ddot{\phi}_M+\frac{l_{M1}}{I_{KM}}K_8(z_7-z_8)+\frac{l_{M1}}{I_{KM}}D_8(\dot{z}_7-\dot{z}_8)-\frac{l_{M1}}{I_{KM}}K_6(z_5-z_6)-\frac{l_{M1}}{I_{KM}}D_6(\dot{z}_5-\dot{z}_6)$$

$$-\frac{2l_{M2}^2K_{13}}{I_{KM}}(\phi_M-\phi_F)-\frac{2l_{M2}^2K_{13}}{I_{KM}}(\phi_M-\phi_R)=0$$

COUPLING EQUATIONS

$$\ddot{z}_6=\ddot{z}_M-l_{M1}\ddot{\phi}_M \qquad \dot{z}_6=\dot{z}_M-l_{M1}\dot{\phi}_M \qquad z_6=z_M-l_{M1}\phi_M$$

$$\ddot{z}_8=\ddot{z}_M+l_{M1}\ddot{\phi}_M \qquad \dot{z}_8=\dot{z}_M+l_{M1}\dot{\phi}_M \qquad z_8=z_M+l_{M1}\phi_M$$

FIGURE A11D. DERIVATION OF EQUATIONS - ROLL PLANE (Cont'd)
(MAIN MODULE)

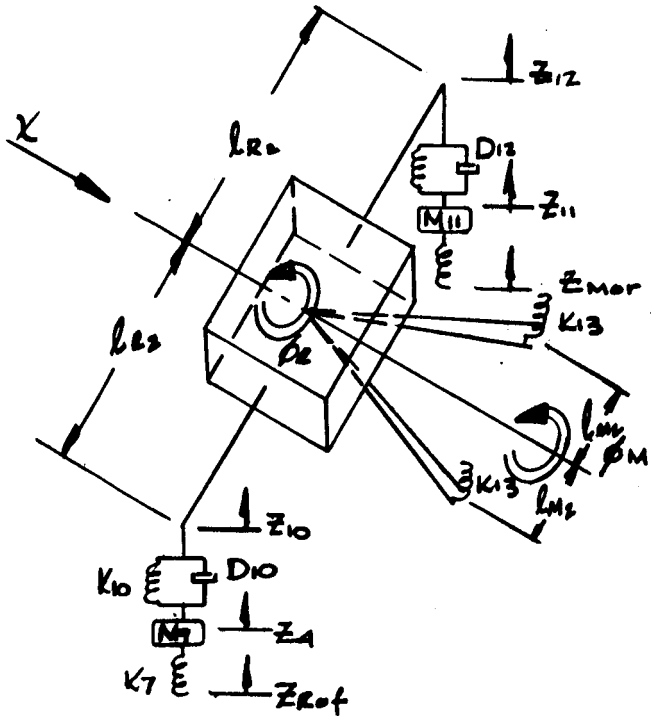

WHEEL EQUATIONS

$$-\ddot{z}_9 + \frac{K_9}{M_9}(z_{Rof} - z_9) + \frac{D_9}{M_9}(\dot{z}_{Rof} - \dot{z}_9) - \frac{K_{10}}{M_9}(z_9 - z_{10}) - \frac{D_{10}}{M_9}(\dot{z}_9 - \dot{z}_{10}) - g = 0$$

$$-\ddot{z}_{11} + \frac{K_{11}}{M_{11}}(z_{Ror} - z_{11}) + \frac{D_{11}}{M_{11}}(\dot{z}_{Ror} - \dot{z}_{11}) - \frac{K_{12}}{M_{11}}(z_{11} - z_{12}) - \frac{D_{12}}{M_{11}}(\dot{z}_{11} - \dot{z}_{12}) - g = 0$$

BODY EQUATION - DISPLACEMENT

$$-\ddot{z}_R + \frac{K_{10}}{M_R}(z_9 - z_{10}) + \frac{D_{10}}{M_R}(\dot{z}_9 - \dot{z}_{10}) + \frac{K_{12}}{M_R}(z_{11} - z_{12}) + \frac{D_{12}}{M_R}(\dot{z}_{11} - \dot{z}_{12}) - g = 0$$

BODY EQUATION - ROTATION

$$-\ddot{\phi}_R + \frac{l_{R2}K_{12}}{I_{xR}}(z_{11} - z_{12}) + \frac{l_{R2}D_{12}}{I_{xR}}(\dot{z}_{11} - \dot{z}_{12}) - \frac{l_{R2}K_{10}}{I_{xR}}(z_9 - z_{10})$$

$$- \frac{l_{R2}D_{10}}{I_{xR}}(\dot{z}_9 - \dot{z}_{10}) + \frac{2l_{M2}^2 K_{13}}{I_{xR}}(\phi_M - \phi_R) = 0$$

COUPLING EQUATIONS

$$\ddot{z}_{12} = \ddot{z}_R + l_{R2}\ddot{\phi}_R \qquad \dot{z}_{12} = \dot{z}_R + l_{R2}\dot{\phi}_R \qquad z_{12} = z_R + l_{R2}\phi_R$$

$$\ddot{z}_{10} = \ddot{z}_R - l_{R2}\ddot{\phi}_R \qquad \dot{z}_{10} = \dot{z}_R - l_{R2}\dot{\phi}_R \qquad z_{10} = z_R - l_{R2}\phi_R$$

FIGURE A11E. DERIVATION OF EQUATIONS - ROLL PLANE (Cont'd) (REAR MODULE)

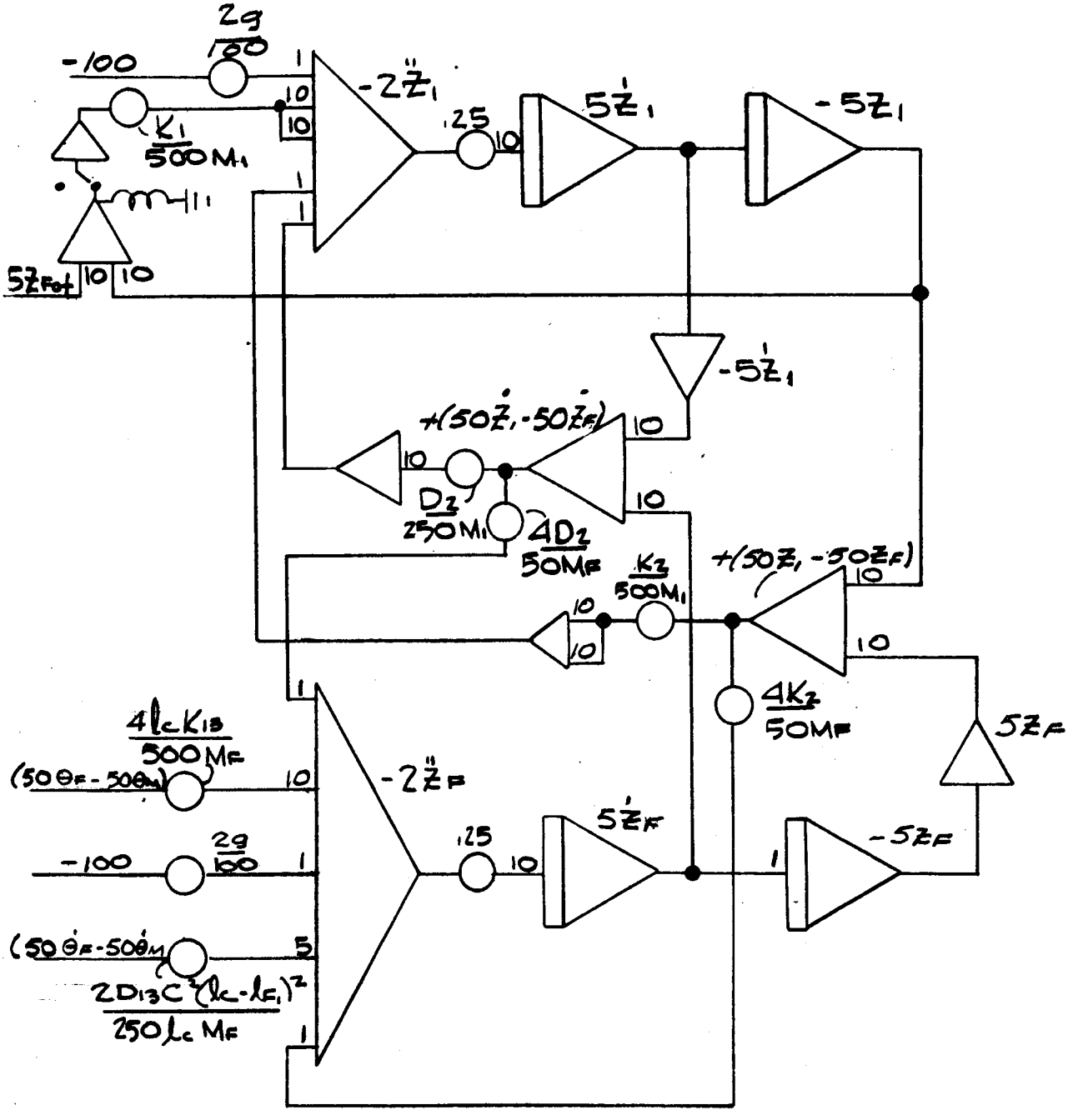

FIGURE A12A. COMPUTER DIAGRAM - PITCH PLANE
(FRONT MODULE)

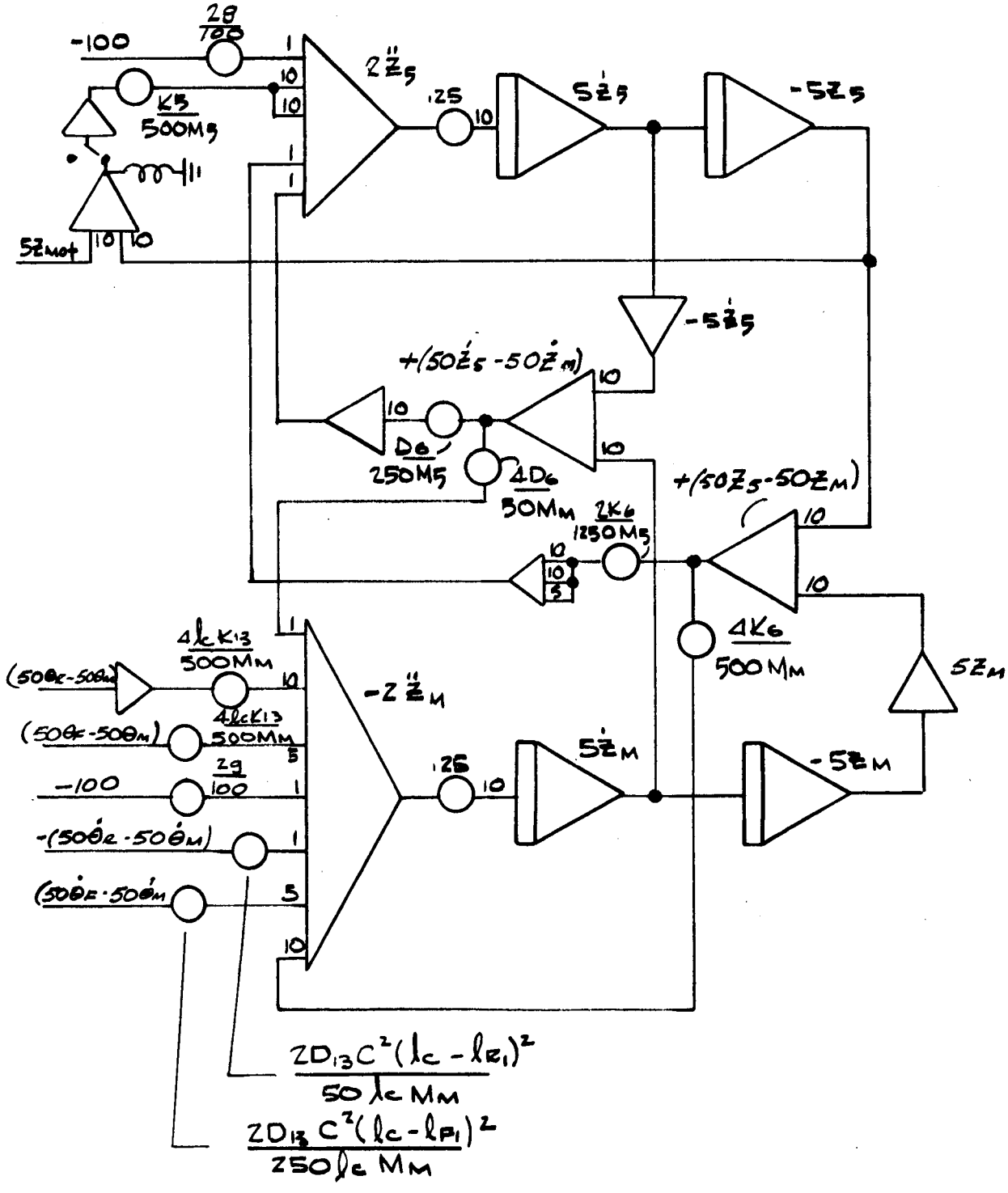

FIGURE A12B. COMPUTER DIAGRAM - PITCH PLANE (Cont'd)
(MAIN MODULE)

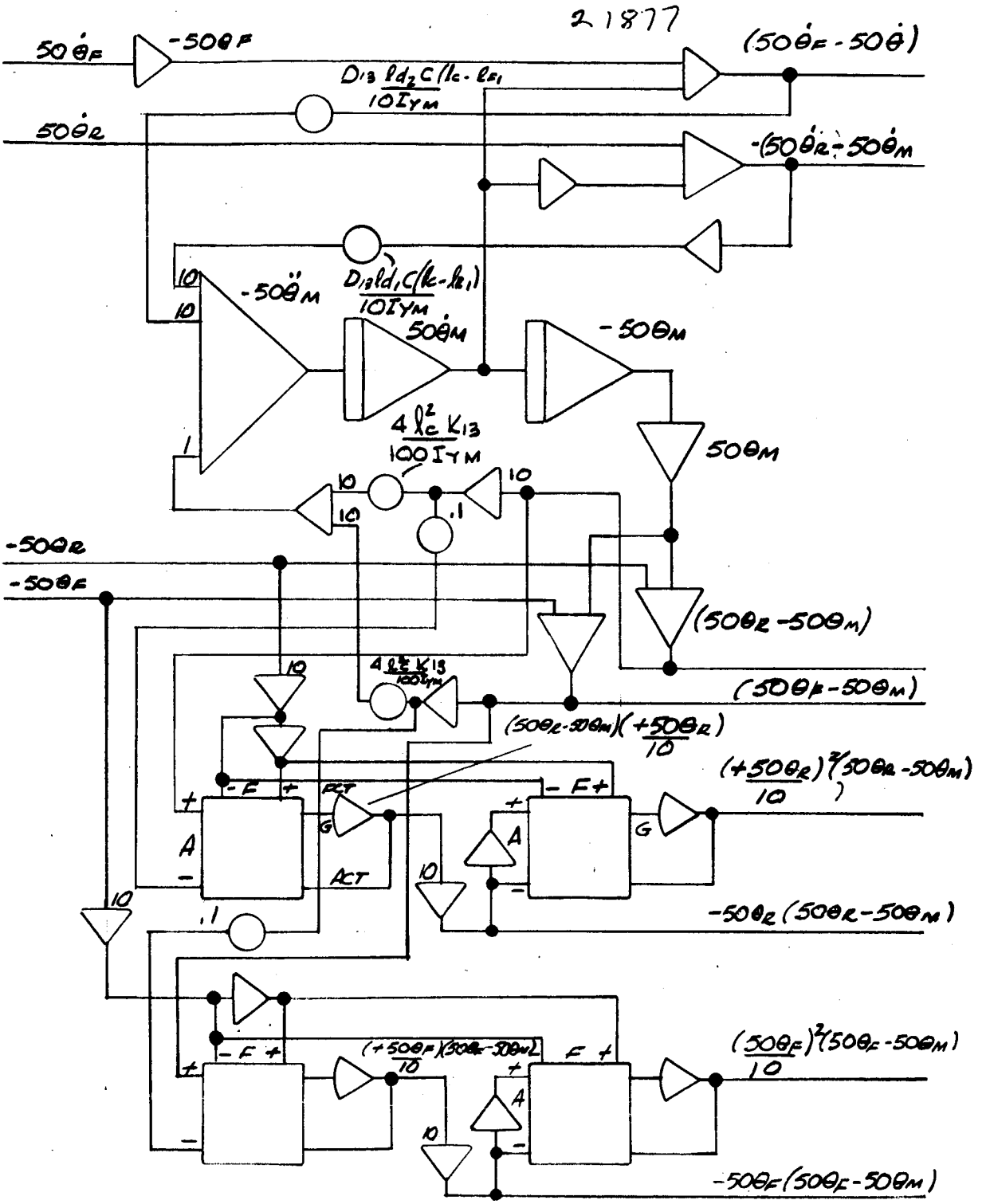

NOTE : INPUT POLARITIES OF QUANTITIES ARE REVERSED ON "F" TO OBTAIN "+" OUTPUTS FROM MULTIPLIERS

FIGURE A12C. COMPUTER DIAGRAM - PITCH PLANE (Cont'd)
(MAIN MODULE)

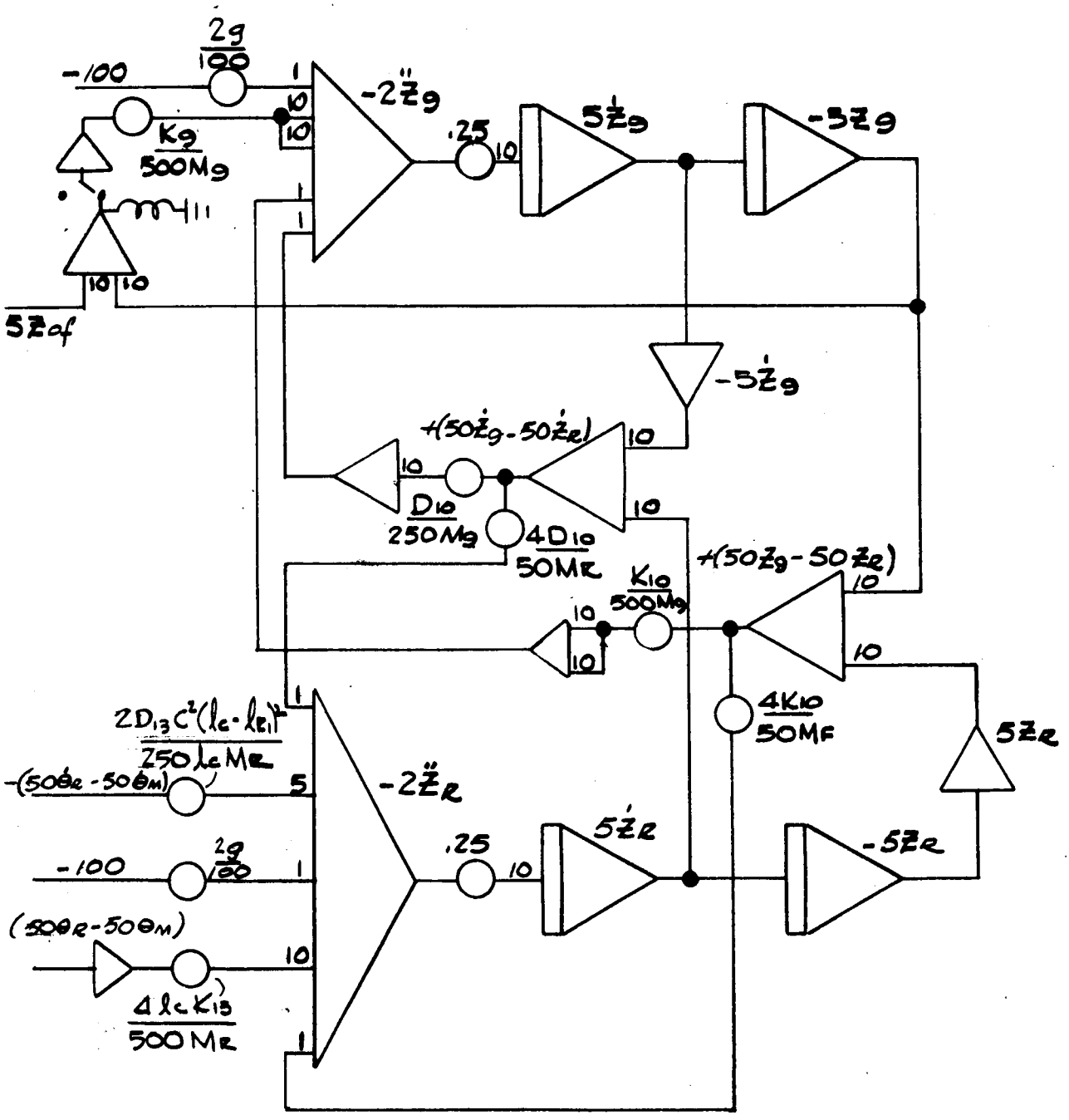

FIGURE A12D. COMPUTER DIAGRAM - PITCH PLANE (Cont'd)
(REAR MODULE)

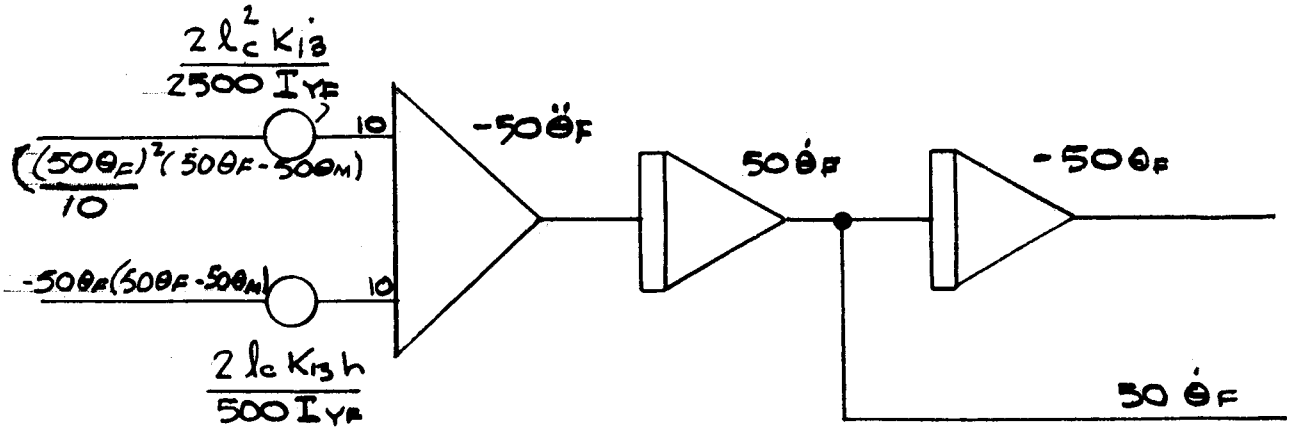

FRONT MODULE

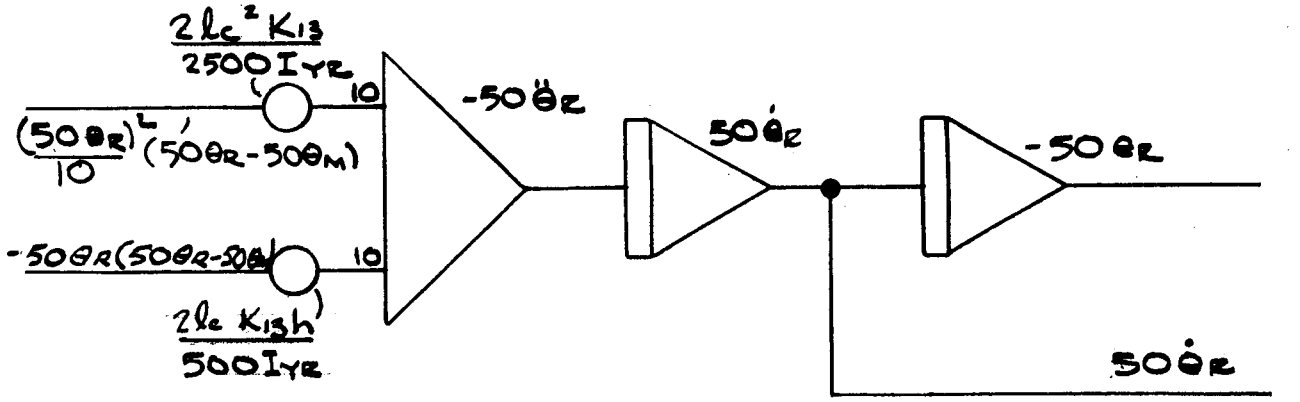

REAR MODULE

FIGURE A12E. COMPUTER DIAGRAM - PITCH PLANE (Cont'd)

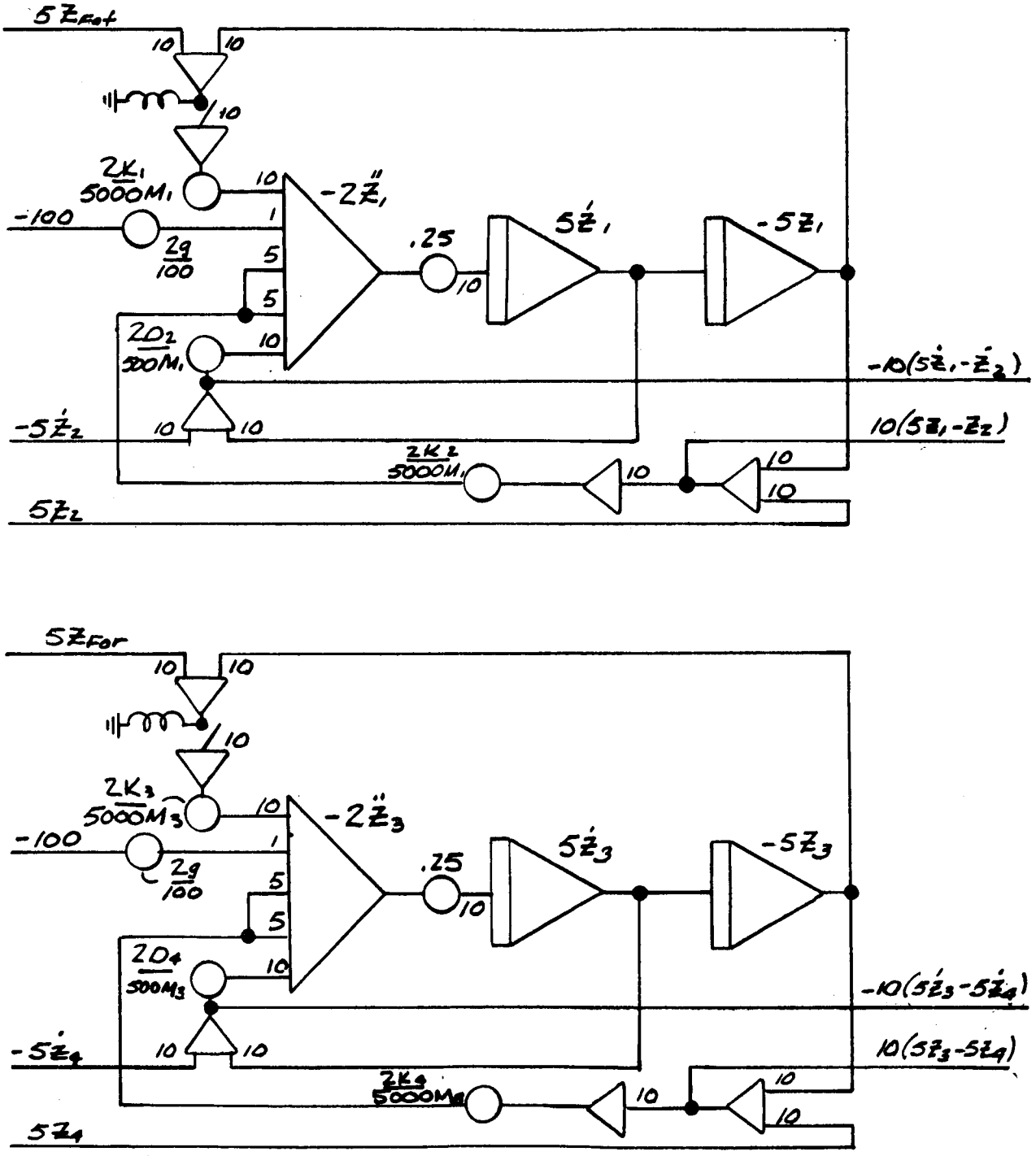

FIGURE A12F. COMPUTER DIAGRAM - ROLL PLANE (FRONT MODULE)

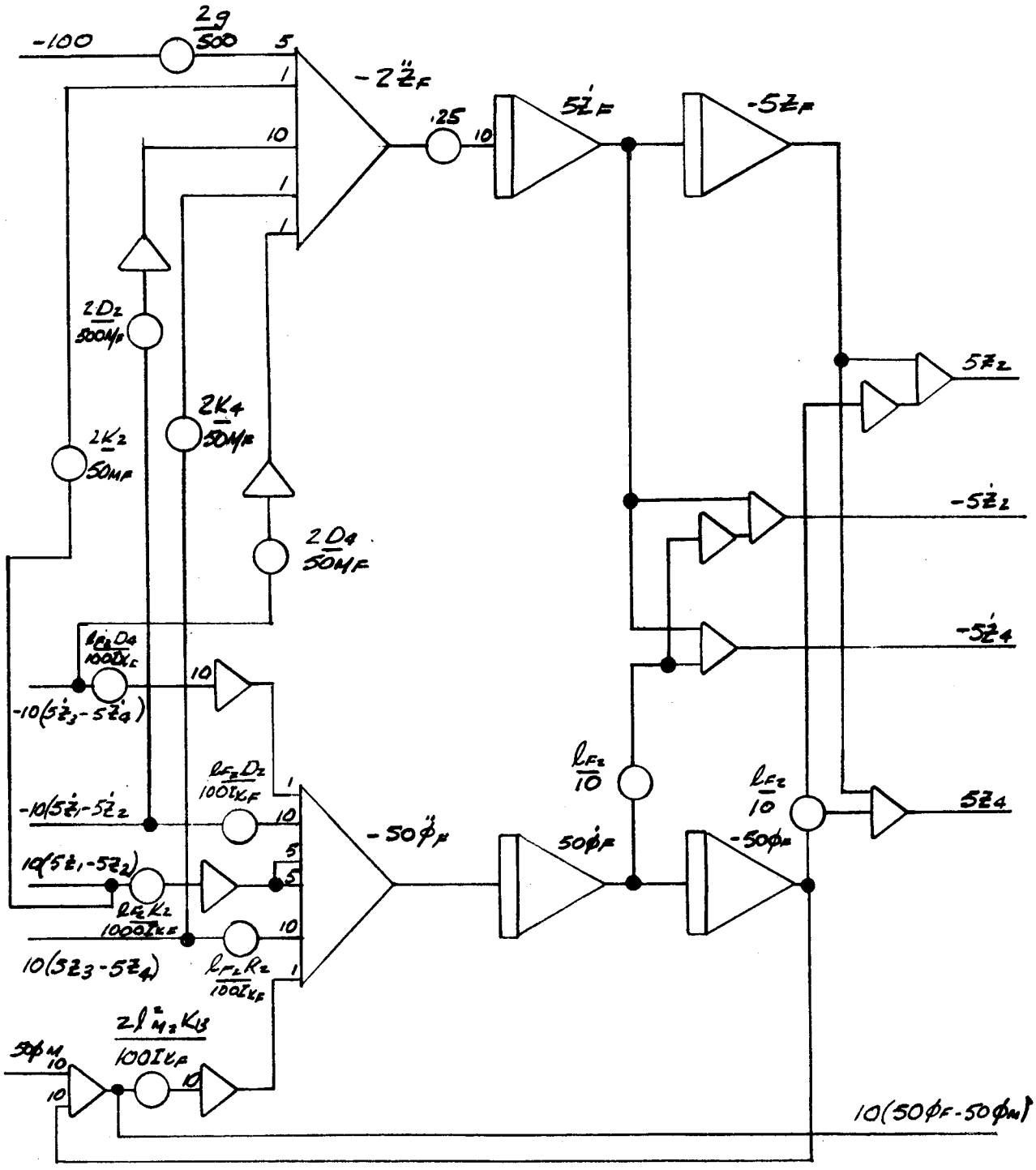

FIGURE A12G. COMPUTER DIAGRAM - ROLL PLANE (Cont'd)
(FRONT MODULE)

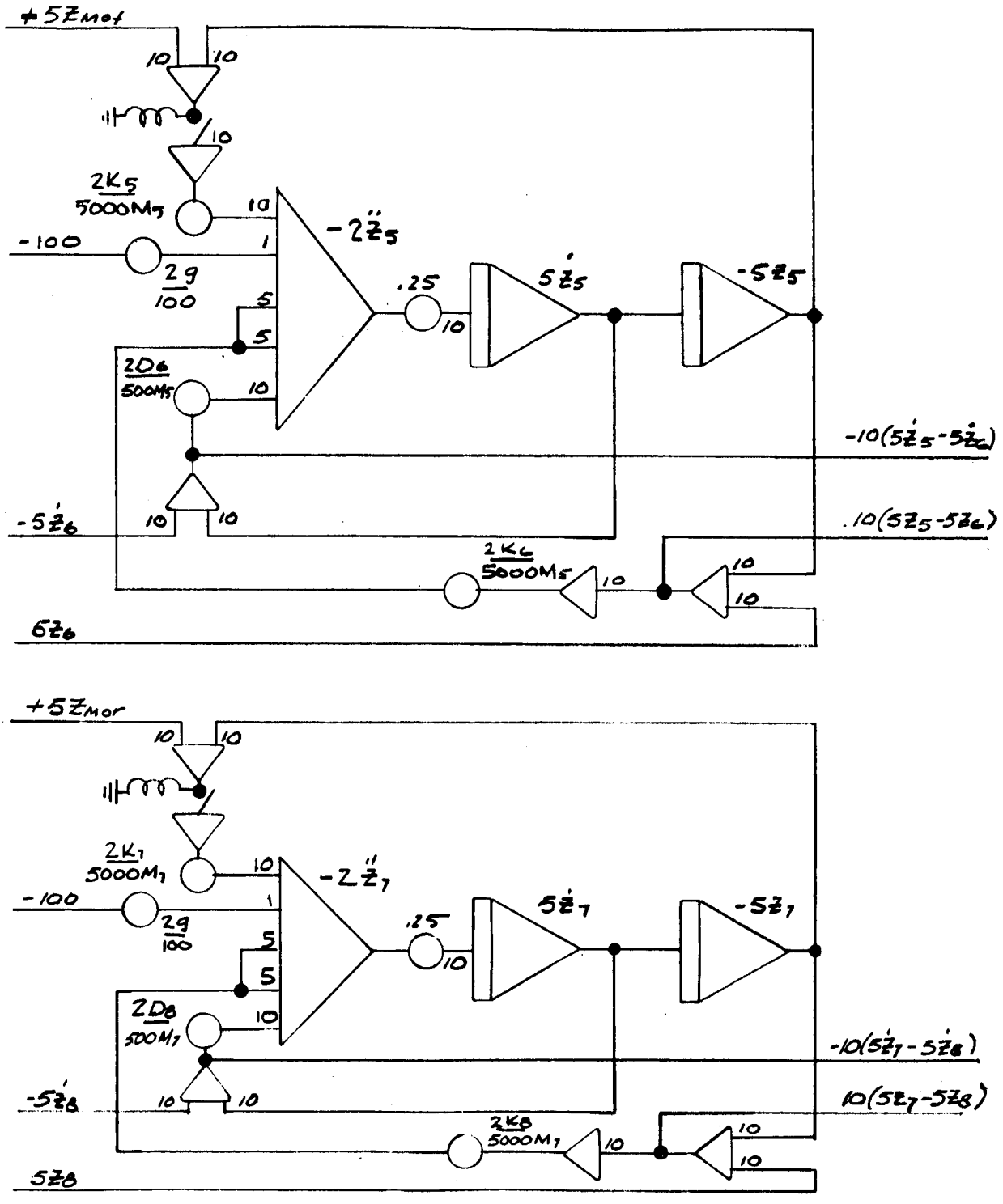

FIGURE A12H. COMPUTER DIAGRAM - ROLL PLANE (Cont'd)
(MAIN MODULE)

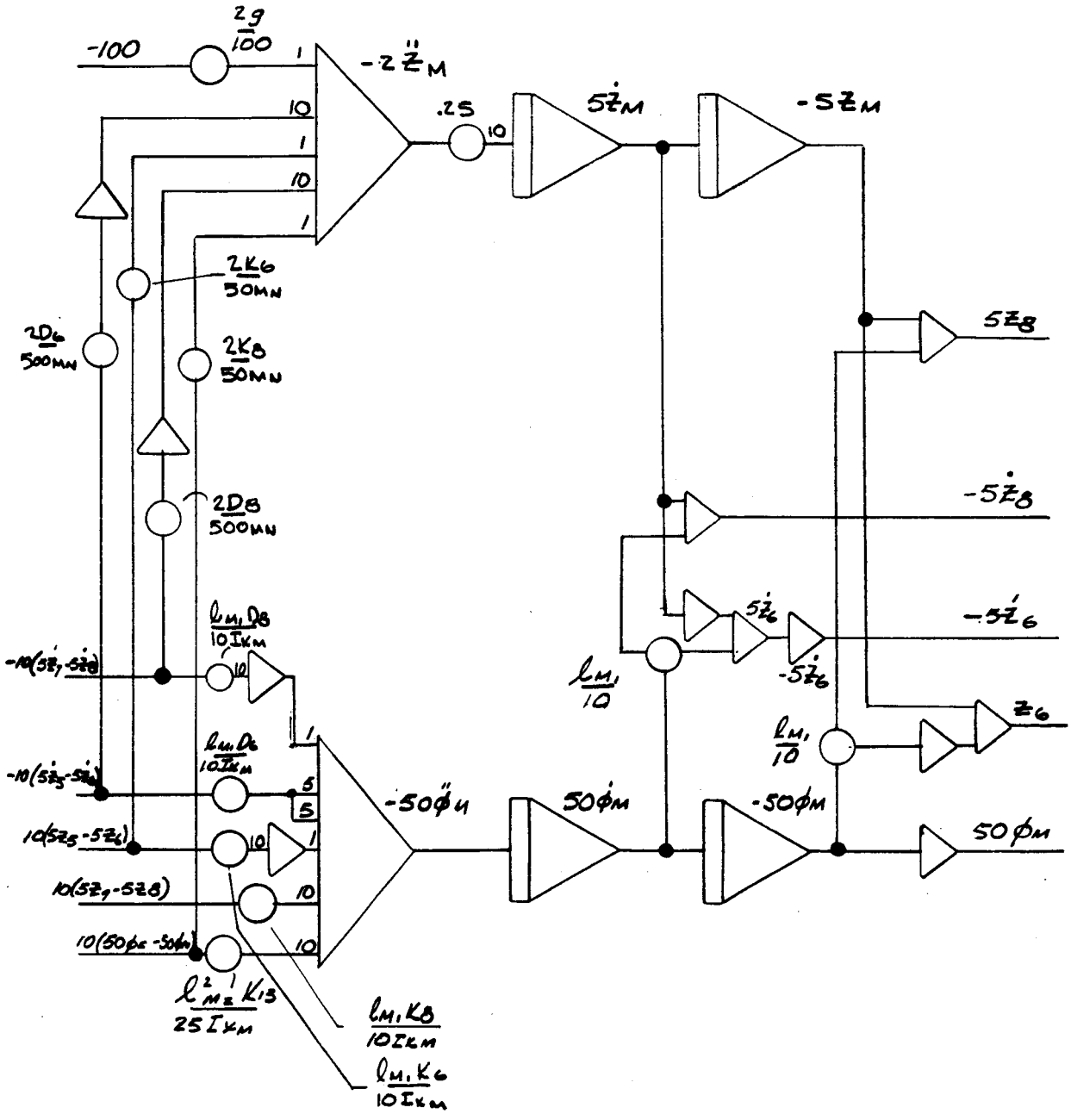

FIGURE A12I. COMPUTER DIAGRAM - ROLL PLANE (Cont'd)
(MAIN MODULE)

SECTION 5.0

REFERENCES

1. Apollo Logistics Support Systems Molab Studies , "Mission Command and Control," Bulletin 006, A. W. Meagher, H. Ryland, September 1964.

2. Apollo Logistics Support Systems Molab Studies, "Task Report on Mobility Systems Analysis," Bulletin 004, E. R. Miles, T. Andrison, August 19, 1964.

3. M. G. Bekker, "Mobility of Cross-Country Vehicles - Part 2 Flotation and Motion Resistance" Machine Design, Volume 31, Number 26, December 24, 1959.

DISTRIBUTION

INTERNAL

DIR
DEP-T
R-AERO-DIR
-S
-SP (23)
R-ASTR-DIR
-A (13)
R-P&VE-DIR
-A
-AB (15)
-AL (5)
R-RP-DIR
-J (5)
R-FP-DIR
R-FP (2)
R-QUAL-DIR
-J (3)
R-COM -DIR
R-ME-DIR
-X
R-TEST-DIR
I-DIR
MS-IP
MS-IPL (8)

EXTERNAL

NASA Headquarters
MTF Col. T. Evans
MTF Maj. E. Andrews (2)
MTF Mr. D. Beattie
R-1 Dr. James B. Edson
MTF William Taylor

Kennedy Space Center
K-DF Mr. von Tiesenhausen

Northrop Space Laboratories
Huntsville Department
Space Systems Section (5)

Scientific and Technical Information Facility
P.O. Box 5700
Bethesda, Maryland
Attn: NASA Representative (S-AK/RKT) (2)

Manned Spacecraft Center
Houston, Texas
Mr. Gillespi, MTG
Miss M. A. Sullivan, RNR
John M. Eggleston

Donald Ellston
Manned Lunar Exploration Investigation
Astrogeological Branch
USGS
Flagstaff, Arizona